



Review article

Recent advances and historical developments of high voltage lithium cobalt oxide materials for rechargeable Li-ion batteries

Kai Wang^{a,b,1}, Jiajia Wan^{a,1}, Yuxuan Xiang^a, Jianping Zhu^a, Qianyi Leng^a, Meng Wang^b, Leimin Xu^b, Yong Yang^{a,c,*}

^a Collaborative Innovation Center of Chemistry for Energy Materials, State Key Laboratory for Physical Chemistry of Solid Surface, Department of Chemistry, College of Chemistry and Chemical Engineering, Xiamen University, Xiamen, 361005, China

^b Ningde Amperex Technology Ltd, Ningde, 352100, China

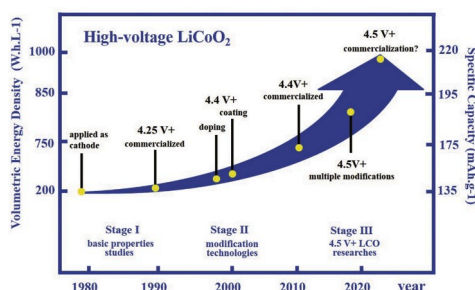
^c School of Energy, Xiamen University, Xiamen, 361005, China



HIGHLIGHTS

- The R&D of LCO cathodes in the last 40 years have been reviewed.
- Three developing stages based on the application voltage of LCO are overviewed.
- LCO modifications and underlying mechanisms are classified and discussed.

GRAPHICAL ABSTRACT



ARTICLE INFO

Keywords:

Cathode
Lithium cobalt oxide
Lithium-ion battery
Modification methods
Doping
Coating

ABSTRACT

One of the big challenges for enhancing the energy density of lithium ion batteries (LIBs) to meet increasing demands for portable electronic devices is to develop the high voltage lithium cobalt oxide materials (HV-LCO, >4.5V vs graphite). In this review, we examine the historical developments of lithium cobalt oxide (LCO) based cathode materials in the last 40 years. According to the research topics at different periods, three research and developing stages of LCO are classified and elaborated. At the first stage, the researches on the basic properties of LCO are comprehensively summarized, which includes crystal/electronic structure, phase changes, electrochemical process, and failure mechanism. At the second stage, the elegant development of modification methods, which aim at improving the stability of the bulk structure, thermal and interface, are introduced in detail. The third stage started from 2018, high capacity (>190 mAh g⁻¹), highly stable and high-rate capability of LCO is being developed and expected to be commercialized in the next few years. Finally, some perspectives of the remaining challenges, as well as the promising applications of HV-LCO, are also discussed.

* Corresponding author. Collaborative Innovation Center of Chemistry for Energy Materials, State Key Laboratory for Physical Chemistry of Solid Surface, Department of Chemistry, College of Chemistry and Chemical Engineering, Xiamen University, Xiamen, 361005, China.

E-mail address: yyang@xmu.edu.cn (Y. Yang).

¹ These authors contributed to the work equally and should be regarded as co-first authors.

<https://doi.org/10.1016/j.jpowsour.2020.228062>

Received 18 January 2020; Received in revised form 7 March 2020; Accepted 15 March 2020

Available online 1 April 2020

0378-7753/© 2020 Elsevier B.V. All rights reserved.

1. Introduction

Lithium ion batteries (LIBs) are dominant power sources with wide applications in terminal portable electronics. They have experienced rapid growth since they were first commercialized in 1991 by Sony [1] and their global market value will exceed \$70 billion by 2020 [2]. Lithium cobalt oxide (LCO) based battery materials dominate in 3C (Computer, Communication, and Consumer electronics)-based LIBs due to their easy procession, unprecedented volumetric energy density, and high operation potential [3–8]. It was first applied as cathode material in rechargeable LIB by Goodenough in 1980 [9], which was of great significance to the history of LIBs including the innovation of oxide-based cathode material to get the operate voltage over 4.0 V, and the application of lithiation anode with no longer employing of lithium metal, which greatly improved the safety of LIBs. The theoretical capacity of LCO with completely lithium removal is about 274 mAh g^{-1} . However, for a long time, the upper-limit charging voltage of LCO based LIBs was limited below 4.25 V, with the capacity of $\sim 135 \text{ mAh g}^{-1}$, which only made use of $\sim 50\%$ of the total capacity [10–12]. Even though the operation voltage of LCO based full cells is improved to 4.45 V today, and the volume energy density is developed from 200 to 700 Wh L^{-1} [12–14]. It is still far from the requirement of practical applications especially considering the expensive price of LCO due to the scarce Co reserves. Therefore, enhancing the energy density of LCO to meet the market demands is still imperative for thinner, lighter, shape flexible portable electronic products, especially smart phones [9,11–13,15,16].

To realize such a goal, diverse strategies have been proposed and developed, including enhancement of compacted densities of the particles, adjustment of the mass ratio of active materials and less use of inactive materials such as binders and current collectors in the composite electrodes, promoting of operation voltage of LCO (see Fig. 1). Up to now, the compacted density and the inactive materials' ratio almost approached their limit, while the practical capacity of LCO is still far from the theoretical value. Therefore, it should be remarkable to increase the energy density by promoting charging voltage than the other strategies. For example, Amatucci et al. [17] isolated the end member of Li_xCoO_2 by removing the lithium ions completely, the CoO_2 , which would convert immediately from a hexagonal single-layered phase O1 to a three-layered O3 Li_xCoO_2 phase at discharge process, and 95% of lithium could be reinserted back into the initial structure and cycle reversibility could be maintained at 4.2 V. Therefore, developing HV-LCO is still attractive and essential to both the academic studies and the industry applications. However, the LCO electrodes would be unstable at high potential and a rapid deterioration of the capacity of LCO-based cells would take place. As shown in Fig. 2, the modified LCO based half cells display outstanding cycling and rate performance when the LCO electrode is at a potential of 4.5 V. Nonetheless, when the potential of the LCO is at 4.6V and 4.7V, the electrochemical performance decrease dramatically [18].

Recently, LCO has attracted much attention and several review articles of LCO based materials appeared periodically in the journals in respect of surface coating, elemental doping, electrolyte modification, and fading mechanisms. For example, Li et al. [8] summarized the development of LIBs based on the evolution of material science over the past 30 years. Wang et al. [12] presented a well-organized review paper of LCO based cathode materials. They comprehensively discussed the whole battery system of LCO based LIBs including the cathode materials, separators, and binders, etc.

In the term of time scale, we can roughly divide the development of LCO into three stages. The first stage is from the 1980s to the early 21st century, the researchers mainly focused on the study of basic properties of LCO [7,10,11,19–25], including physical/chemical properties, crystal structures as well as electronic properties of LCO during lithium ions' (de)intercalation processes. The HV-LCO at that time was referred to as the operating voltage higher than 4.25 V. In this case, the monoclinic phase transition was the main origins which deteriorate the HV

performance of LCO. The second stage is 2001–2018, during this time scale which the structure and surface stability of LCO at the higher voltage ($>4.25\text{V}$) become the main research focus. Consequently, elemental substitution and surface modification of LCO have made big progress [2,26–36]. The upper cut-off voltage was increased and the definition voltage of HV-LCO became 4.4 V at that time. The third stage starts in 2018. Generally speaking, developing $4.5 \text{ V} + \text{LCO}$ brings more serious challenges [37–40], such as the irreversible phase transition, the surface side reactions, the decomposition of electrolyte, etc. Nowadays, the definition of HV-LCO would change again to $4.5 \text{ V} + \text{LCO}$ based cathode materials. Although a few works about 4.5 V LCO have been reported, few of them have demonstrated effective methods to realize higher voltage applications of LCO, and much more efforts should be paid to reach such a goal.

The high-voltage stable electrolyte is also necessary for the HV-LCO applications. Solvents in the routine electrolytes would be oxidized at high potential ($>4.3\text{V}$ vs Li). For example, intensive electrolyte side reactions will occur during high-voltage cycling, leading to an unstable electrode/electrolyte interface with a dramatic increasing of the CEI layer, which can accelerate the fatigue of the battery [41]. Apart from the development of high-voltage liquid electrolyte with functional additives, solid-state electrolytes with wide electrochemical window can be attractive in the future application of HV-LCO. Solid-state LCO-lithium batteries combined with lithium metal anodes is also a promising candidate for next-generation high-energy batteries.

In addition, developing compatible cathode materials to replace LCO is also essential. For example, Ni-based layered materials such as $\text{LiNi}_{1/2}\text{Mn}_{1/2}\text{O}_2$, $\text{LiNi}_{1/3}\text{Co}_{1/3}\text{Mn}_{1/3}\text{O}_2$, $\text{LiNi}_{0.85}\text{Co}_{0.1}\text{Al}_{0.05}\text{O}_2$, etc. show comparable electrochemical performance but with lower price have been already widely used in LIBs such as electric vehicles [42–44]. They become more competitive in specific energy density with increasing content of Ni, and could be one of the best candidate materials to replace LCO in some applications [45].

In this paper, we outlook the historical development of LCO based cathode materials during the last 40 years from an electrochemical viewpoint. The understanding of the relationship between and structural/interfacial evolution and electrochemical performance of LCO are emphasized. The recent advances in the research of electrochemical processes and phase changes with increasing upper cut-off voltage as well as capacity/voltage failure mechanism analysis are reviewed.

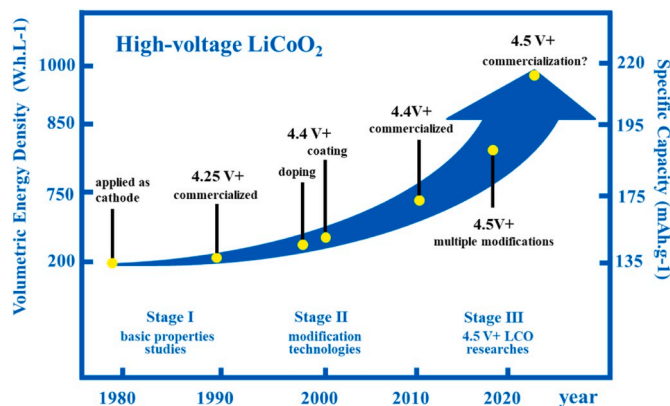


Fig. 1. The historical development roadmap of cutoff voltage of LCO-graphite full cells. Volumetric Energy Density (VED) and specific capacity of LCO materials are both listed as Y-axis. The Volumetric Energy Density is estimated from available LCO-graphite pouch cells.

2. Physicochemical properties and electrochemical failure analysis of LCO

2.1. Crystal structure of LCO

In the early 1980s, Armand [46] firstly put forward the concept of “Rocking Chair Battery” based on the solid solution electrode. At the same time, LCO came into the secondary battery field [9]. Unfortunately, LCO did not attract much attention until its commercialization after ten years. Many scientists including Dahn, Ceder, Tarascon, Delmas, Cho, et al. carried out many insightful studies of LCO for its various physicochemical properties, which included the crystal structures, powder conductivities, electronic properties, phase transitions during lithium (de)intercalation process, and some mechanism studies such as lithium/vacancy order-disorder arrangement.

LCO crystal adopts the α -NaFeO₂ type layered structure (rhombohedral space group $R\bar{3}m$) with alternately arranged CoO₂ and LiO₂ layers. The cobalt atoms and the lithium atoms reside respectively in the 3a and 3b sites with ordering in alternate octahedral coordination in (111) plane and the oxygen atoms occupy the 6c site with a ccp packed stacking. Such a structure of LCO can also be regarded as an “O3 structure”, in which the letter “O” indicates that Li occupies an octahedral site, and the “3” gives the number of CoO₂ sheets in a one-unit cell [47]. Another form of LCO was firstly discovered by Delmas and called O2-type LCO with AB CB AB oxygen packing that was metastable compared with O3-LCO which showed AB CA BC oxygen packing [47]. The structure of this material (noted O2) is described in a hexagonal unit cell having space group $P6_3mc$ with $a = 2.8036 \text{ \AA}$ and $c = 9.5372 \text{ \AA}$ and

shows that CoO₆ octahedra shares one face and three edges with LiO₆ octahedra while the O3 phase shares six edges [48–50].

At the early stages of LCO research, intensive research and efforts have been devoted to understanding the physical and chemical properties of Li_xCoO_2 ($0 \leq x \leq 1$). In particular, structural variation, conduction mechanism, electronic evolution, a preliminary understanding of capacity fade and so on were the research hotspots. Dahn et al. [51] firstly studied the crystal structure of LCO during charging up to 4.35 V through in-situ X-ray diffraction (XRD) in 1992, and they discovered the monoclinic (M1) phase transition at about 50% lithium removal in LCO (Fig. 3a). Then in 1994, Ohzuku et al. [52] further studied the crystal structure of LCO to 4.5 V with a combination of in-situ XRD and electrochemical methods, and found the phase transition voltage at about 4.5 V, about 80% lithium removal. They suggested it was the second monoclinic (M2) phase transition process which could lead to a structure shrinkage along the c axis of the LCO crystal and deteriorate the performance of LCO based batteries.

As shown in Fig. 3b, a series of in-situ XRD researches demonstrate that the crystal structure of LCO would experience a series of phase transitions during (de)intercalation process, which includes O3-1/H1 phase, O3-2/H2 phase, monoclinic (M1) phase, O3/H3 phase, M2/H1-3 phase, and O1 phase. Among them, the O3-2/H2 phase is similar to the O3-1/H1 phase with a tiny distinction in the symmetry of the transition metals. The M1 phase belongs to $C2/m$ space group, in which Li occupies the 2a and 4c sites, Co resides at the 2b and 4c sites, and O occupies the 4c sites. The H1-3 phase is a hybrid structure of the rhombohedral form of LCO and CoO₂, in which the Li is assumed to occupy the 3a sites with the Co and two O atoms occupy the 6c sites

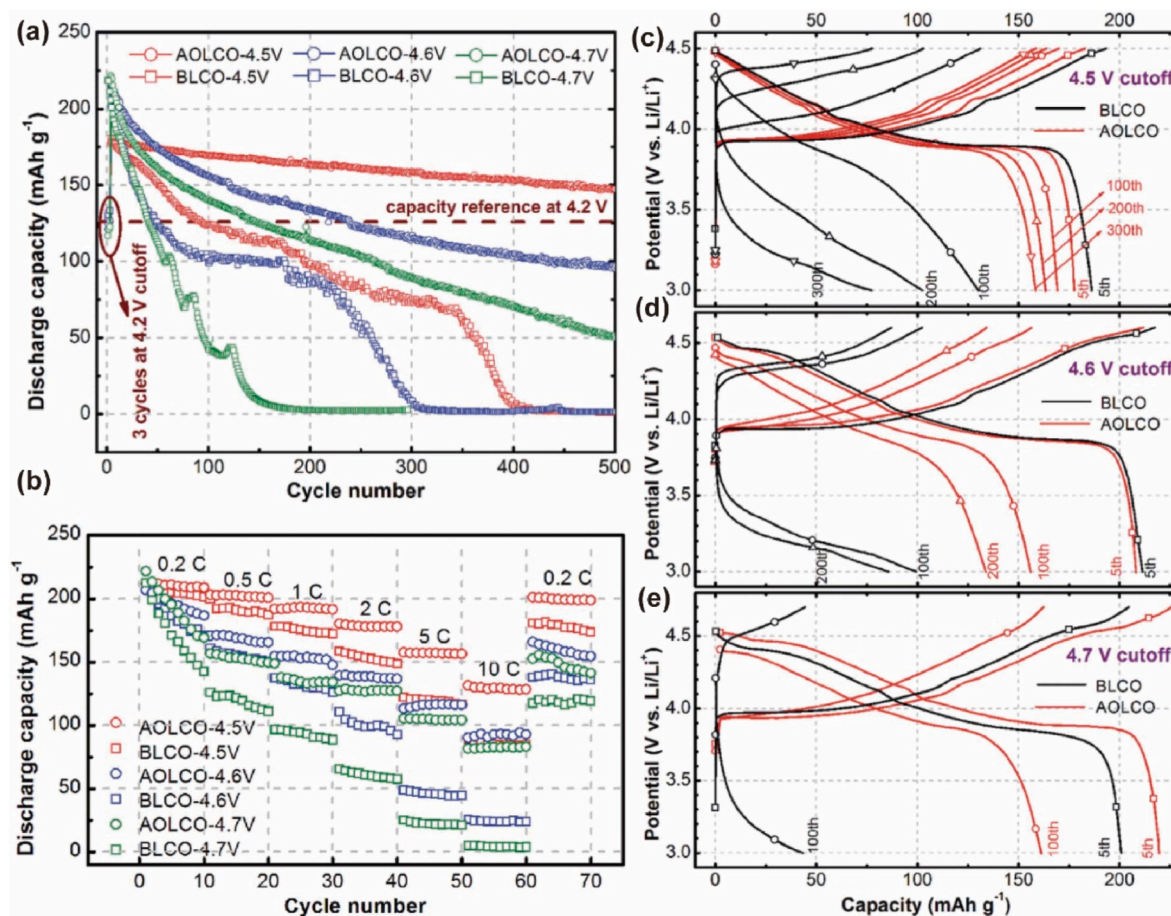


Fig. 2. Electrochemical performances of bare LiCoO₂ (BLCO) and Al₂O₃-coated LiCoO₂ (AOLCO) composite electrodes at different potentials from 4.5 V to 4.7 V at 1C and at room temperature (RT). (a) Discharge capacity, (b) Rate performances of the BLCO and ALCO electrodes at different potentials at RT and (c–e) selected charge/discharge profiles at different potentials of the LCO electrodes [18].

(Fig. 3c–d). Finally, the O1 phase would form when Li is completely removed from the LCO, which contains only CoO_2 layers with stacking in ABAB form.

The structural evolution in the process of (de)-intercalation of lithium ions is closely related to performance degradation. With lithium ions de-intercalation, LCO will continuously undergo a sequence of phase transitions in the forms of solid solutions at about 3.93 V, 4.07 V, and 4.19 V (vs. Li/Li^+) respectively [55]. Initially, the insulator-metal transition will occur at a low voltage of about 3.93V, forming a two-phase coexist region in Li_xCoO_2 ($0.75 < x < 0.94$). A phenomenon of (003) diffraction peak split or symmetry variation would be recorded through the in-situ XRD analysis during this process. However, these two phases are similar with only a tiny difference in the lattice parameters. Conductivity measurements and ^7Li NMR results proved that the electronic effect related to the elevation of the cobalt valence was the prime

reason that leads to the phase transition, rather than structural factor [56]. Meanwhile, the repulsion between adjacent layers would increase by degrees during the early lithium removal process, which would cause a gradual increase of the c -axis. With continuous deintercalation of lithium ions, H2 to M1 phase, which was one of the most popular research topics of LCO, would take place at about 4.08 and 4.20 V (vs. Li/Li^+) [52]. This result was validated by different groups with a combination of cyclic voltammetry (CV) and in-situ XRD analysis [51]. Besides, the vacancy order-disorder theory was proposed and proved afterward through first-principle calculations [57]. When approximately half of Li^+ was removed from the LCO, the host structure experienced a lattice distortion, which would lead to a change of the spatial distribution of Li ions and Li vacancies [57]. This would drive a phase transition from the hexagonal to the monoclinic structure. However, this phase transition is reversible, and the monoclinic structure would turn

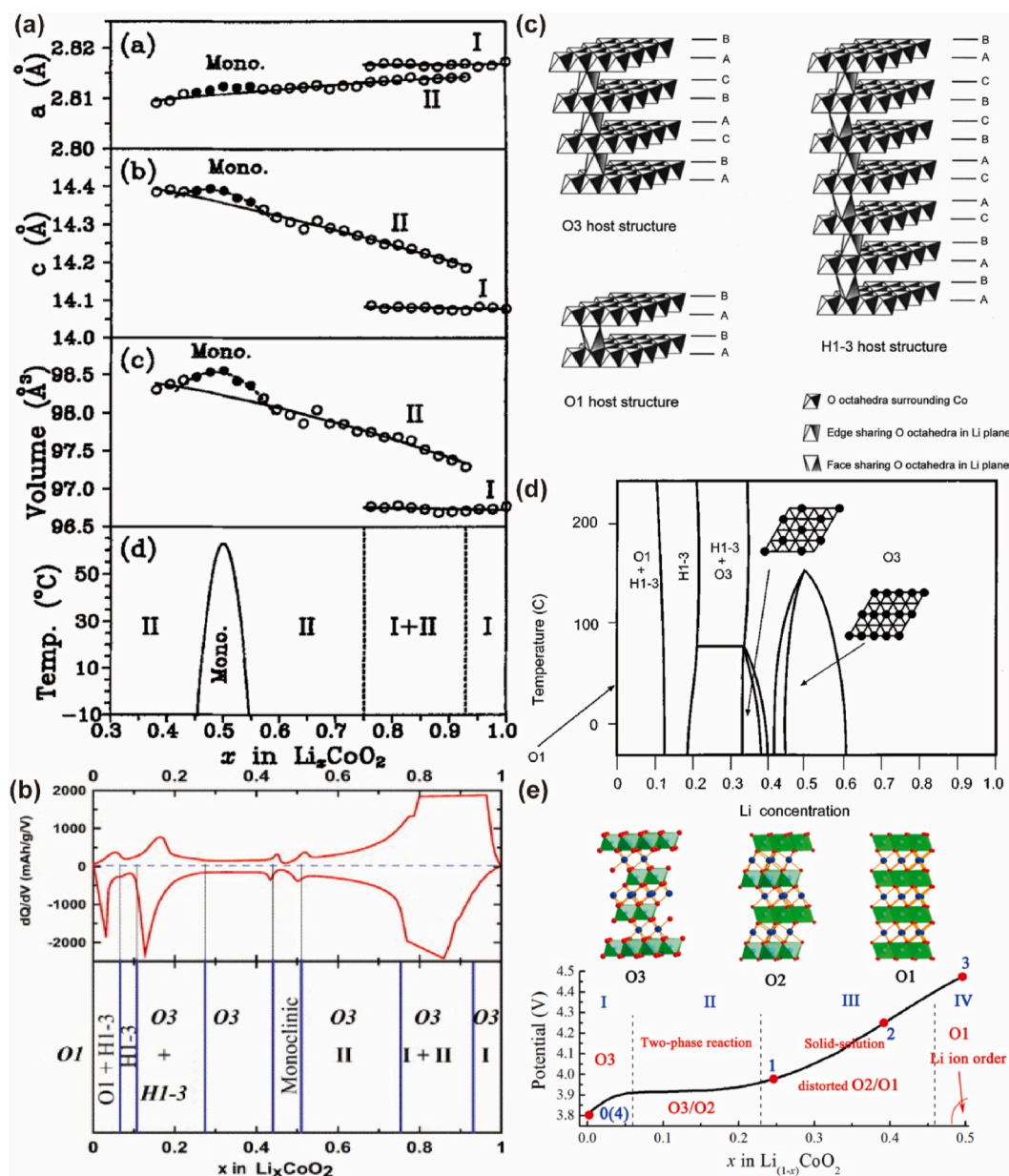


Fig. 3. (a) Unit cell constants a , c and cell volume as a function of lithium concentration x in Li_xCoO_2 . Combined with the global phase diagram for Li_xCoO_2 [51]; (b) Differential capacity vs. Li concentration in Li_xCoO_2 and phase diagram of Li_xCoO_2 [20]; (c and d) Schematic illustration of the three host structures O3, O1, and H1-3 and the calculated Li_xCoO_2 phase diagram. The insets show the in-plane Li ordering predicted to be stable at $x = 1/2$ and $1/3$ [53]; (e) Phase diagram of $\text{Li}_{(1-x)}\text{CoO}_2$ ($0 \leq x \leq 0.50$) nanoparticle. Numerical symbols 0–4 represent the sample points for STEM observation: (0) pristine LiCoO_2 , (1) charged to ca. 3.9 V, (2) charged to 4.2 V, (3) charged to 4.5 V, and (4) back to 3.0 V [54].

back to hexagonal soon with lithium reinsertion. Delma et al. [58] suggested that the monoclinic distortion was caused by the shearing of the rhombohedral oxygen lattice through the electron diffraction patterns. The monoclinic phase transition of LCO at about 4.2 V has been considered to be the main culprit to the degradation of the LIBs and referred to as the bottleneck that hindered the development of HV-LCO for a long time. However, there was no solid evidence to support such a point of view. Firstly, the monoclinic phase transition is reversible. Although commercial cell experiences many cycle numbers, the monoclinic phase transition still presents until battery failure. Secondly, some works draw a conclusion that the monoclinic phase transition of LCO exerts little influence on cycle performance. Claude Delmas [59,60] claimed that over-stoichiometric $\text{Li}_{1.08}\text{CoO}_2$ sample didn't have the monoclinic transition in the galvanostatic charge curves, but it would appear after undergoing the annealing treatment about 5–10 days at 900 °C. They ascribed this phenomenon to that the excess lithium was removed by the high temperature heating process for a long time. In addition, the electrochemical performance was not affected by the absence of monoclinic phase transition. These results indicate that the monoclinic transition is relevant to Li/Co ratio and almost not negative

to the cell performance.

Another phase transition of Li_xCoO_2 ($0 < x < 0.25$) at HV over 4.5 V was first discovered by Ohzuku et al. [52]. They demonstrated that the *c*-axis of LCO would go through a serious collapse, which was considered to be the Jahn–Teller distortion of CoO_6 octahedra [58]. After that, Ceder's [61] group also investigated the phase stability in the layered Li_xCoO_2 at low Li concentration ($x < 0.4$) through the first principles calculation, which investigated a sequence of phase transitions at HV as following [62]. Firstly, the H1-3 phase was indicated as a hybrid host structure between the rhombohedral LCO and the hexagonal CoO_2 ; Secondly, the O3, as well as the H1-3 phase, coexisted when the lithium content was $0.19 < x < 0.33$, and the H1-3, as well as the O1 phase, coexisted when the *x* was less than 0.12; Finally, when the *x* was between 0.12 and 0.19 in Li_xCoO_2 , the phase could stay stable. All the calculated conclusions were subsequently demonstrated again with several corresponding experiments. Two-phase transitions occurred at 4.55 V and 4.63 V, corresponding to the transition from the O3 phase to the H1-3 phase and then to the O1 phase, were confirmed through a combination of the voltage profile of Li/LiCoO₂ cells, the differential capacity vs. voltage curves, and the in situ XRD data [24]. The end

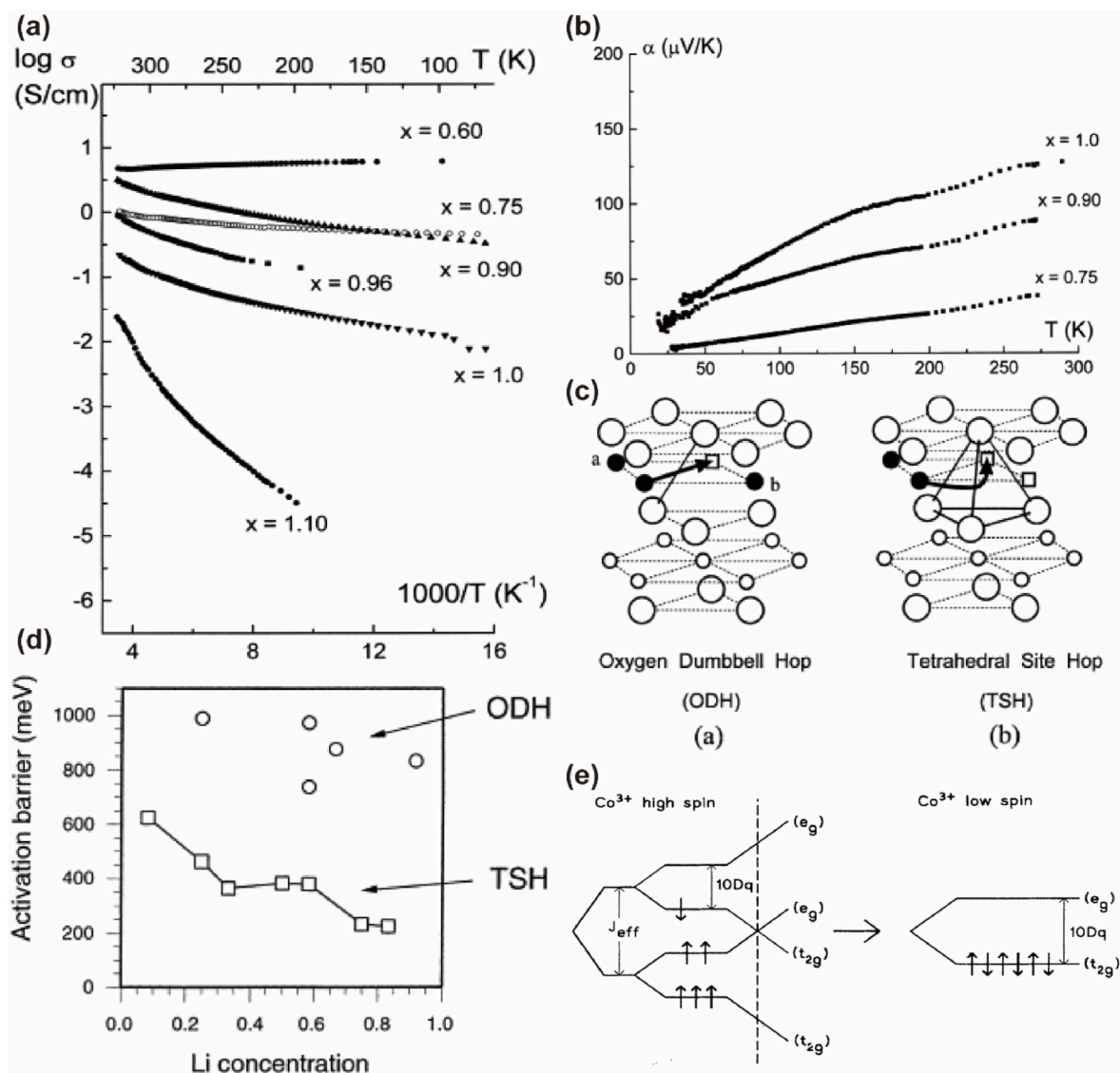


Fig. 4. (a–b) Variation of the logarithm of the electrical conductivity vs. reciprocal temperature of Li_xCoO_2 ($x_0 = 1.10$) deintercalated samples ($0.60 \leq x \leq 1.10$) and Thermal variation of the Seebeck coefficient of Li_xCoO_2 ($x_0 = 1.10$) deintercalated samples ($0.75 \leq x \leq 1.0$) [60]. (c–d) The two lithium migration paths in Li_xCoO_2 ; Activation barriers for the ODH TSH mechanism at different Li concentrations [69]. (e) The change in the ordering of the Co^{3+} d orbitals in going from high spin (left) to Low spin (right) [70].

member of LCO with a complete lithium deintercalation was reported by Tarascon's group, which was realized with the help of an ingenious designed in-situ electrochemical device [17]. It was the first time to isolate the O1 phase, the CoO_2 , from the electrochemical deintercalation reaction system for LCO. Li's group discovered that the O2- Li_xCoO_2 could be formed after the first electrochemical lithiation investigated by spherical aberration correction and advanced STEM-HAADF techniques while previous results showed that there was merely O3-stacking [54]. It was the first report of a conversion mechanism that existed between the O2 type and O3 type LCO, and the O2 type LCO was only obtained via exchange reactions reported before. They deduced that the phase transformation from the O3 phase to O2 type in $\text{Li}_{1-x}\text{CoO}_2$ nanoparticles first existed during the process of $0.07 < x < 0.25$ with a two-phase reaction. Then was the appearance of the O2/O1 solid solution at $x = 0.43$, referred to as the distorted crystal structure. Finally, the transformation of O2 to O1 phase was completed at $0.43 < x < 0.52$. The transformation process was also demonstrated in Fig. 3e.

The structural variation would have a profound effect on electrochemical properties for LCO. Relative researches were performed to study this issue. Especially, the LCO based LIBs would undergo a rapid capacity fading at HV over 4.5 V with irreversible structure degradations. On the one hand, relative changes in the volume of the LCO crystal due to the sequence phase transitions from the O3 to the H1-3, and to the O1, which would accumulate crystal strains. On the other hand, the particles were highly unstable at HV with a lack of pillars in lithium layers, and the Co ions were at a relatively high oxidation state as well. As a result, undesirable crystal surface slips and partial elemental dislocations would take place immediately, and led to the deterioration of the cathode [63]. In a word, although high capacity retention could keep after one cycle for LCO at high voltage up to 4.8V, the capacity fading will quickly take place at long-cycle applications. It is still very tough to apply LCO at HV (>4.5V), and the irreversible O3→H1-3→O1 phase transitions over 4.5 V remain an urgent technical bottleneck to overcome.

2.2. The physical and chemical properties of LCO

The physical and chemical properties of the cathode material LCO, such as electronic conductivity, ionic diffusion, electronic structure and so on, are the key factors that determine the electrochemical performance. Among them, the electronic conductivity and lithium-ion diffusion coefficient are considered to be the dominant parameters that induce extensive study for in-depth understanding and promotion strategy of them [23,64–68].

The high electronic conductivity of LCO ($\sim 1 \times 10^{-3} \text{ S cm}^{-1}$) was reported at room temperature, which is ascribed to the formation of a small concentration of Co^{4+} ions with a certain density of electron holes and the inevitable Li defects during the high-temperature synthesis process [71]. Therefore, LCO allowed a very high discharge rate of Li/LCO cells [72]. Besides, the electronic conductivity of pure LCO at a given temperature increased with the oxygen partial pressure, consistent with the peculiarity of p-type semiconducting oxide [73]. As shown in Fig. 4a–b, the (de)lithiated compounds of Li_xCoO_2 present the conductivity of an activated nature, high values of thermoelectric power and the positive value of the Seebeck coefficient, which reveals the presence of electron-hole for charge carriers and so exhibited p-type semiconducting behavior [60,74]. Upon a de-lithiation process, a strong increase in both the electronic conductivity and thermoelectric power demonstrates the presence of an insulator-metallic phase transition, which may originate from the delocalization of localized electrons that in the neighborhood of Co ion [56]. On the basis of this mechanism, various methods were proposed to improve the electronic conductivity. For instance, the excessive lithium and the incorporation of Mg could put up the valence of Co^{3+} , thus, producing electric holes to improve conductivity [71,75].

The lithium-ion diffusion coefficient of the LCO was determined to be

10^{-11} to $10^{-7} \text{ cm}^2 \text{ s}^{-1}$ and the average diffusion coefficient of de-lithium compound Li_xCoO_2 was in the range of $10^{-9} \text{ cm}^2 \text{ s}^{-1}$, implying the relatively facile diffusion dynamics of LCO [65,76]. Van der Ven et al. [69] put forward two kinds of diffusion paths of lithium ions and calculated corresponding activation barriers by the local vacancy arrangement. The first diffusion mechanism was called oxygen dumbbell hop (ODH) that lithium-ion migrated through the initial site of the hop and vacancy with the shortest distance when the endpoint of the hop was adjacent to two lithium sites (site a and b in Fig. 4c). The second diffusion mechanism was called tetrahedral site hop (TSH) occurred when the endpoint of the hop was near the vacancy and lithium passed through a tetrahedral site with a divacancy mechanism. Fig. 4d shows the relationship between the calculated activation barriers and Li concentration, which displayed the larger value of activation barriers of the ODH mechanism compared to the TSH mechanism. This reveals that lithium diffusion predominately mitigated through a tetrahedral site with a divacancy mechanism. Besides, the diffusion coefficient varied over several orders of magnitude at different lithium content due to diverse activation barriers. To improve lithium-ion diffusion, diverse strategies have been proposed. Among which, substituting Co ion with larger radius ion is an effective way due to the enlarged interlayer spacing, which is always called “pillar effects”. For instance, the replacement of Co^{3+} (54.5 nm) by La^{3+} (103.2 nm) could enlarge inter-lamellar spacing, which is conducive to the deintercalation of lithium ions [77].

It is well known that the electrochemical behavior of cathode strongly depends on the electronic structure of the material. Thus, extensive attentions are focused on the electronic structure of LCO and its evolution during the cycling process in the literature reports, which is commonly investigated by x-ray photoemission spectroscopy (XPS), x-ray-absorption spectroscopy (XAS) and theoretical calculations. X-ray emission spectroscopy and XPS results show that the valence band of oxygen 2p and cobalt 3d orbitals of LCO in its ground state was mixed, giving LCO a fairly large covalent mixture [78]. The main electronic state of LCO was proved to be low-spin Co^{3+} states with so localized d-electrons, probably due to the strong enough crystal field created by the small Co–O bond length [70] (Fig. 4e). This strong crystal field could maintain the origin electronic state of Co from the interference of other doping trivalent elements. For example, the doping limit of $\text{LiFe}_x\text{Co}_{1-x}\text{O}_2$ solid solution was $x = 0.25$, where cobalt ions were still in low-spin Co^{3+} ($S = 0$) and iron ions were high-spin Fe^{3+} ($S = 5/2$) configurations [79]. However, McLaren argued that Fe ions in $\text{LiFe}_x\text{Co}_{1-x}\text{O}_2$ were determined to be a $3+/4+$ mixed-valence state and occupied 6c sites, which would block fast Li conduction in the Li layer, leading to the disordered structure upon charging process [80]. Also, the presence of oxygen defects/vacancies with some crystal field non-homogeneity was inevitable, which induced by mechanochemical wear from such as ball mill mixing of original material and uneven oxygen loss on the surface at high-temperature synthesis process. The oxygen 1s spectra in XAS and one-electron model results displayed that the O 1s and O 2p had almost a similar density of states, so the correlation effects of 3d band were too small to be detectable [81]. However, in the vicinity of the Fermi level, the density of states exhibited relatively high values with the bandgap of 2.7 eV, displaying the property of charge-transfer insulator of LCO [78].

The electronic structure of the de-lithiation compound has also been discussed. One point of view deemed that removing Li ions from LCO led to change the electronic structure of Co and transfer electron holes into the valence band, which caused the Fermi level downwards, leading to an insulator-metal phase transition. In addition, the electronic structure of oxygen would vary after lithium removal. Montoro [82] examined the electronic structure of LCO and its chemical de-lithium compounds by using Co 2p and O 1s XAS as well as calculations of atomic multiplet and band structure. They found that O ions were reduced upon de-intercalation while Co ions remained trivalent Co^{3+} low-spin state. Moreover, The oxygen K-edge XANES results suggested that the holes compensating due to the de-intercalation of LCO are located primarily in

the oxygen 2p states rather than in the Co 3d states [83]. A similar phenomenon is observed in the chemical de-lithium samples of $\text{Li}_{1+x}\text{CoO}_2$ and it also showed the characteristics of electron de-location [84]. Nevertheless, another new opinion about the electron transfer mechanisms upon lithium deintercalation was put forward by Gonbeau et al., in 2008 [85]. Through analyzing all available XPS core peaks and valence spectra, they hold the view that both cobalt and oxygen would simultaneously participate in holes compensating resulting from Li^+ extraction and the possibility of solo engagement of oxygen atom was out of the question.

The introduction of other elements into crystal structure would exert influence on the electronic structure of materials. For instance, tetravalent ion doping like Ti^{4+} would cause the generation of defections that is related to the doping amount. A small amount of Ti^{4+} doping for $\text{LiTi}_{0.01}\text{Co}_{0.99}\text{O}_2$ led to the occurrence of Co^{2+} observed by the XANES spectra. However, the increase of Ti^{4+} contents up to $\text{LiTi}_{0.25}\text{Co}_{0.75}\text{O}_2$ induced the appearance of Co^{4+} due to the inhomogeneous distribution of Ti ions in the LCO host crystal [86]. What's more, although the trivalent doping ion has the same valence state as the Co ion in LCO, it can still affect the electronic structure, ordering and defect/vacancy of the host crystal. Yoon et al. [87] performed an XAS study of $\text{LiAl}_{0.25}\text{Co}_{0.75}\text{O}_2$ and found the Al addition would cause a larger local structure distortion during lithium removal than bare LCO. This larger structure distortion may be responsible for the rapid capacity fading of the $\text{LiAl}_{0.25}\text{Co}_{0.75}\text{O}_2$. Moreover, the substitution of Al for Co ions in LCO leads to more increased oxygen participating in charge compensation during the charging process by analysis of the spectral changes of the Co L-edge and O K-edge XAS [88]. $\text{LiCo}_{1-y}\text{B}_y\text{O}_2$ ($y < 0.25$) compounds could also be indexed with the rhombohedral R-3m space group, indicating B incorporation didn't change the layer structure of LCO. However, it decreased the crystalline of LCO concluded by the broadening of X-ray diffraction line and the absence of a splitting of the (006) (102) and (108) (110) Bragg lines. Besides, due to the considerable difference between ionic radii of B^{3+} and Co^{3+} , $\text{LiCo}_{1-y}\text{B}_y\text{O}_2$ samples possess the enhancement of cation ordering [89]. As for low valence ions doping like Mg^{2+} with larger size compared to Co^{3+} . The mechanism of charge compensation is still on debate. The one was the creation of Co^{4+} ions sharing an itinerant electron-hole with neighboring Co III ions [89]. The other was the presence of intermediate spin state $\text{Co}^{3+}(\text{IS})$ ions adopted MgO_5 square-based pyramidal environment with oxygen vacancies [90]. Besides, over-stoichiometry LCO, $\text{Li}_{1+x}\text{CoO}_2$, also attracts much attention for exploring electronic structure variation and thus produces three kinds of opinions. Firstly, Carewska et al. [75], Peeters et al. [91] and Delmas et al. [60] found the existence of paramagnetic Co^{2+} species with the low-spin configuration in $\text{Li}_{1+x}\text{CoO}_2$. In more recent work in 2014, Ogumi et al. [92] proved it again and thought that the produced low spin Co^{2+} was not associated with the oxygen vacancy based on NMR results. Secondly, other view is that the excess lithium doping in nonstoichiometric $\text{Li}_{1+x}\text{CoO}_2$ ($0 < x < 0.1$) samples don't lead to the reduction of Co^{3+} to Co^{2+} , but appeared a new state of oxygen ions different from lattice oxide through the X-ray, IRS, XPS, EDRS and magnetic measurements results [84]. Thirdly, Levasseur et al. [60] deduced that the excess Li ion occupied the Co site, and the resulting charge deficit was compensated by both the oxygen vacancies and the decline of Co valence state.

2.3. The electrochemical failure mechanism analysis

Although LCO-based lithium-ion batteries have been commercialized since 1991, the further application of LCO is obstructed by the capacity/voltage decay, in particular, at prolonged cycle number in the initial period. Up to the time around 2000, various fundamental mechanisms were proposed to explain the cause of capacity decay as follows: (i) The deteriorating structure induced by a series of phase transitions upon charge/discharge process, was responsible for the capacity decay. It was generally believed that the monoclinic phase transition was the culprit

of battery deterioration, which can be mitigated by suppressing or eliminating this phase transition. (ii) surface chemistry was the direct cause of capacity decay. The formation and accumulation of surface films, as well as the change of surface component or structure, greatly deteriorated the cycle performance.

As previously reported, surface chemistry plays a major role in cell life. Kim [93] found that the bulk structure of electrode materials in the 18650-type batteries was almost unchanged after long cycles. However, the significant increase in impedance of batteries and exfoliation of active materials from the current collector was observed. Thus, the gradually increasing impedance was ascribed to the formation and accumulation of LiF-rich CEI/SEI layer, which resulted in the sluggish dynamics of the electrochemical process and failure of the batteries at last [94]. There was a debate as to whether battery failures occur primarily at the cathode or anode. For one thing, impedance data revealed the dominance of impedance at the cathode side after 800 charge-discharge cycles, which demonstrated the cathode issues were the culprit of capacity fade [95,96]. However, Popov [97] found that the increase in the discharge rate would accelerate the deterioration of cell capacity. At high discharge rates (3C), the whole capacity loss mainly roots in the carbon anode, which was highly related to the increasing surface film resistance at the anode. This is different from the mechanism at low rate discharge. Dahn et al. [98] explored the aging mechanisms using LCO/Graphite cells with different cycling histories in a range of 0.3–12 years through high precision coulometry measurements combined with electrochemical impedance spectroscopy and differential voltage analysis. The results demonstrated that capacity fade dominantly took place in the graphite anode due to the continuous formation of SEI, which gradually consumed the active lithium and resulting in detriment of resistance and a large amount of irreversible capacity. Dahn et al. [99] put forward another view about the performance decay mechanism. Compared with surface modification samples, the heat-treatment step alone LCO also displayed good cyclic stability even though voltage was up to 4.5 V. They thought that surface species formed by the exposure of LCO in the air were detrimental to the cell performance. Thus, removing these surface species by the pre-heating step in the coating process could improve the capacity retention during cycling to 4.5 V. Besides, aging mechanisms were in connection with the cycle condition such as temperature, charge/discharge protocol, current density and so on. These factors could deteriorate capacity, which was ascribed to aggravated loss of active Li^+ , active material (LCO/graphite exfoliation) and rate capability [100].

The surface structure and composition of LCO also alter with cycling. For example, Chiang [101] et al. employed TEM to investigate the surface structure of cycled LCO, by which they observed the fractured particles, cation disorder and high density of extended defects. Moreover, through the selected-area electron diffraction, two types of cation

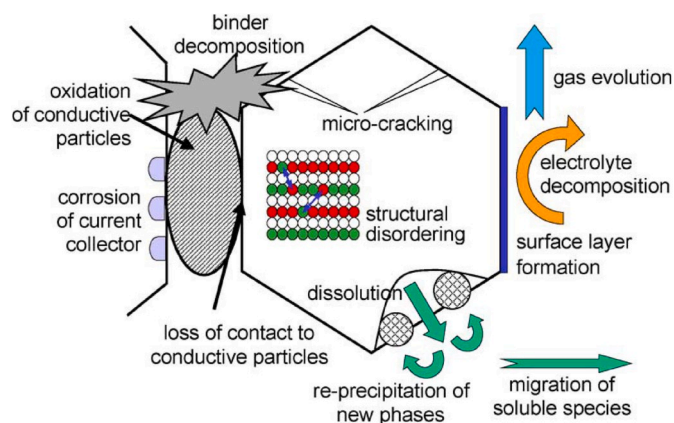


Fig. 5. Diagram of basic electrochemical aging mechanisms of cathode materials [104].

disorder were observed, which were ascribed to the exchange of Li and Co from corresponding layers due to partial transformation of spinel tetrahedral site order respectively. This result, for the first time, revealed the cation deficiency and cycling-induced spinel disorder in LCO material, which were invisible for the bulk X-ray diffraction techniques or neutron diffraction [102].

When charged to a higher voltage ($>4.4\text{V}$), the intensified structural change and severe electrolyte side reactions trigger some new investigations and understanding about the failure mechanism of LCO. On the one hand, the repeated deep Li (de)intercalation at high voltage has caused grievous bulk structure change due to a serious phase transition. Especially, the H3 to H1-3 and O1 phase transitions occurred at about 4.55V and 4.65V respectively have been considered to be the most disruptive factors concerning a large contraction in the lattice volume, which induces internal strain and mechanical grinding. Then, the intergranular and intragranular cracks are formed after prolonged high-voltage cycling. However, there is a lack of effective methods for alleviating the H1-3 and O1 phase transition that occurred at HV, which hinders the further application of HV LCO. On the other hand, cycling at higher voltage dramatically influences the degree of electrolyte degradation, leading to an increase in the complexity and instability of the cathode electrolyte interface (CEI). Interfacial regression has been

identified as a crucial factor for cell failure, which mainly results from the degradation of the CEI layer and the surface phase transformation layer. The unstable CEI layer induced by high-voltage cycling would aggravate the dissolution/reduction of transition metal ions and oxygen instability with gas release at the cathode surface. The quantitative analysis between the percentage of cobalt loss and capacity loss at 4.5V evidenced that the capacity fading was directly related to the amount of cobalt dissolution [19]. Besides, the formation of the cubic spinel phase on the surface degradation layer with an increased density of dislocations and the internal strains are observed in high-voltage cycling LCO material, which seriously impedes the long-term cycle life of cell [103]. Furthermore, the gradually thickening CEI layer may generate an extensive blocking effect for lithium-ion migration together with the suppressed kinetics. Hence, the development of effective electrolyte additives which can stabilize CEI/SEI structure and alleviating electrolyte decomposition is a potentially crucial direction to the high-energy battery.

3. The development of efficient modification methods for LCO

Based on the early stage researches, the crystal structure of pristine LCO as well as the Li_xCoO_2 ($0 < x < 1$) during the charge/discharge

Table 1

Some selected modification methods to realize HV-LCO.

Modification methods	The functions of doping elements and coating layer	Electrochemical performance (LCO/Li)				Ref
		1st discharge capacity (mAh g^{-1})	Capacity retention /cycle No.	Current density	Voltage range/V (vs. Li/Li^+)	
Mn doping; $\text{LiCo}_{0.95}\text{Mn}_{0.05}\text{O}_2$	Mn: improve the structure stability and diffusion rate;	172	87%/100	50 mA g^{-1}	3.0–4.4	[171]
Ni doping; $\text{LiCo}_{0.95}\text{Ni}_{0.05}\text{O}_2$	Ni: suppress the spinel phase formation and improve the stability of the CEI layer	177	93%/100	185 mA g^{-1}	3.0–4.45	[172]
Mg doping; $\text{LiCo}_{0.99}\text{Mg}_{0.01}\text{O}_2$	Mg: improve electronic conductivity and structural stability;	184	79%/55	1 C	3.0–4.5	[173]
Mg, Cu co-doping; $\text{LiMg}_{0.045}\text{Cu}_{0.155}\text{Co}_{0.8}\text{O}_2$	Mg: stabilize the CoO_2 layers; Cu: improve Li^+ conductivity;	197	88%/100	0.2 C	3.0–4.5	[174]
Mg,F co-doping; $\text{LiMg}_{0.05}\text{Co}_{0.95}\text{O}_{1.95}\text{F}_{0.05}$	Mg: increase the inter slab distance; F: improve the thermal and surface stability;	185	88%/50	0.5 C	3.0–4.5	[123]
Al, La co-doping; La: Al: Co = 1:2:1000	La: increase the c axis distance; Al: suppress the monoclinic phase transition; facilitate Li^+ diffusion; stabilize the structure;	190	96%/50	C/3	3.0–4.5	[77]
Al,Ti bulk co-doping and surface Mg doping; doping $<0.4 \text{ wt}\%$	Al and Ti: improve the structure stability; Mg: improve the interfacial stability;	224.9	78%/200	0.5 C	3–4.6	[175]
0.1% wt% Al, Mg, Ti doping;	Al, Mg: suppress the phase transition; Ti: promote lithium diffusion; alleviate internal strain;	220	86%/100	0.5 C	3.0–4.6	[180]
Al_2O_3 coating; 0.5 wt %	Suppress electrolyte decomposition;	180	97%/140	C/3	3.6–4.5	[20]
Li [$\text{Li}_{0.2}\text{Mn}_{0.6}\text{Ni}_{0.2}$] O_2 coating; 5.0 wt %	Suppress the dissolution of Co;	172.8	96.4%/100	0.2 C	3.0–4.5	[147]
$\text{LiAlO}_2/\text{LiCo}_{1-x}\text{Al}_x\text{O}_2$ double-layers coating;	Improve Li^+ conductivity;	178.1	73%/500	180 mA g^{-1}	3.0–4.5	[157]
Olivine LiCoPO_4 coating; coating layer thickness 7 nm	Improve thermal stability;	171	89.4%/50	1 C	3.0–4.5	[146]
Li_3PO_4 coating; coating layer thickness: 60 nm	Improve the surface/interface stability; Improve Li^+ conductivity;	185	80%/100	140 mA g^{-1}	3.0–4.5	[176]
$\text{Li}_4\text{Ti}_5\text{O}_{12}$ coating; 25 nm coating layer	Improve Li^+ conductivity;	190	90%/60	28 mA g^{-1}	3.0–4.5	[36]
2 mol % AlF_3 coating;	Suppress electrolyte decomposition; Reduce Co dissolution; HF-scavenger; Suppress electrolyte decomposition Delay spinel phase transformation;	208	94%/50	0.2 C	3.0–4.54	[159]
LiAlPO_3 coating; 2 wt%	Improve the ionic and electronic conductivity; Suppress electrolyte decomposition;	206	92%/50	100 mA g^{-1}	2.75–4.55	[177]
$\text{Li}_{1/3}\text{Al}_{1/3}\text{Co}_{2/3}\text{O}_{4/3}\text{F}_{2/3}$ coating; 2 wt%	Suppress electrolyte decomposition; Suppresses the phase transition at HV; Improve Li^+ conductivity;	216.2	81.8%/200	27.4 mA g^{-1}	3.0–4.6	[37]
Nano- Al_2O_3 additive; 2.0 wt%	Improve Li^+ conductivity; H_2O -scavenger;	187	85%/100	0.15 mA cm^{-2}	3.3–4.5	[178]
$\text{N}_3\text{P}_3(\text{OPh})\text{F}_5$ additive; 2 vol%	Form the uniform, denser and stable CEI; Improve thermal stability; Suppress electrolyte decomposition;	186	91%/300	140 mA g^{-1}	3–4.5	[179]

process are clarity. Firstly, the stability of the bulk crystal structure is significant to bear the deformation and the stress brought by phase transitions during the cycling process. Secondly, the physical and chemical properties of LCO can also affect the electrochemical performance through slight adjustments on the local electronic structure and the surface of particles. Finally, the interfacial side reactions between LCO and electrolytes can lead to the degradation of batteries and sometimes will bring about potential safety risks. Previous studies of basic aging mechanisms of cathode materials are listed in Fig. 5.

To realize HV-LCO, at that time referred to as the upper cut-off voltage over 4.4 V, the critical challenges are the improvement of the structure and surface stability of LCO. Corresponding strategies including bulk doping and surface modification have been developed to meet such challenges. Ohzuku et al. [5] suggested that introducing metal ions in LCO would enhance the structural stability to extend the cycling ability. While the surface modifications were thought to present as defenses to resist the electrolyte decomposition as well as the attack of HF to enhance the interfacial stability of LCO. Both of the strategies or a combination of them would make sense to the application of LCO at HV, therefore, various efforts were paid during the last two decades to optimize LCO based materials. As a consequence, the upper cut-off voltage of LCO based batteries was elevated to 4.4 V+, some of the typical materials showed excellent electrochemical performance even at 4.5 V. Furthermore, it greatly promotes the update of LCO based LIBs in industry and 4.4 V + LIBs are successfully commercialized in recent years.

The modifications have created new materials through the introduction of foreign atoms into the bulk of LCO or surface coating with other materials. The enhancements of stability properties of the modified materials, including the surface/bulk stability and structure reversibility of LCO based materials, are considered the most essential aspects to achieve HV applications. Typical doping elements such as Al, Mg, and Ti which are effective and are widely used in industry, can greatly help to improve the bulk structural stability of LCO. Surface coating with oxides, such as Al_2O_3 , which can improve the stability of the interface between LCO and electrolyte, is proved successful techniques for modifications. In addition, the physical and chemical

properties of the modified materials would be various to pristine LCO. For example, Mg doping would alter the electronic conductivity of LCO. Functional materials coating, such as fast ionic conductors, are used to enhance the ionic conductivity of LCO. Accordingly, much more attention is paid to regulate such properties of LCO, which are greatly corresponding to the electrochemical performance of batteries.

Some parts of the representative modification methods are selected and summarized in Table 1 including different doping, coating methods and some other modification strategies. The chemical formulas of the modified-LCO materials are also listed with a brief introduction of the modifications, possible working mechanisms to enhance the electronic performance, with corresponding to some essential performances including application voltage, specific capacity cycling performance, etc.

Doping and coating are always discussed respectively with lists of different elements or compounds, followed with discussions of their working functions. Nevertheless, there are numerous reports in the improvement of the modified LCO, and some of the methods are similar in functions. The improvement mechanisms would be much more meaningful to guide and forecast future technologies. Moreover, there is no clear-cut distinction between doping and coating, for example, some elements are not easy to dope without careful adjustments on synthetic methods as well as the amount of the precursors, and would always lead to surface enrichment on the particles; on the other hand, atoms in coated layer would disperse into near-surface to form subsurface doping. In other cases, the surface coating would greatly influence the inner properties of the LCO by removing the exceed lithium in the bulk through reacting with lithium. In a word, the aspects of the improvements of LCO instead of modification methods would be more coherent to understand the development of HV-LCO. Therefore, in this section, we would discuss with classification of material's performance improvement mechanisms instead of modification methods. The performance improvement mechanisms will be divided into three parts, including the structure reversibility, thermal stability, and interface stability.

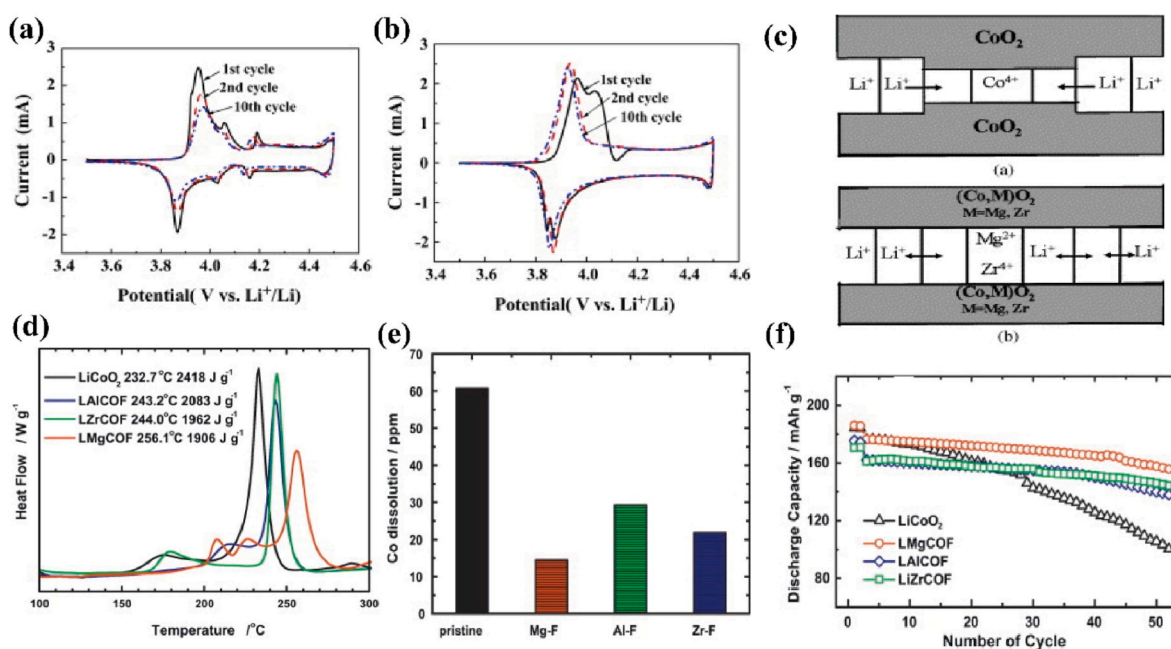


Fig. 6. (a–b) CV of bare LCO and $\text{LiCo}_{0.97}\text{Mg}_{0.03}\text{O}_2$ respectively [114]. (c) Schematic of the pillaring effect of Mg or Zr doping [117]. (d) DSC traces of de-lithiated pristine LCO, F and Mg (LMgCOF), Al (LAlCOF), Zr (LZrCOF), co-doped LCO based electrodes charged to 4.5 V [123]. (e) Amount of Co dissolution of the pristine LiCoO_2 , LMgCOF, LAlCOF, and LZrCOF samples after 7 days storage at 60 °C [123]. (f) Cycling performance of the pristine LiCoO_2 , LMgCOF, LAlCOF, and LZrCOF samples at a current density of 80 mA g⁻¹ (0.5 C-rate) [123].

3.1. Structure stability and reversibility

There are usually two situations of the fading of cathode materials, one is a slow aging process with cumulated active lithium loss through cycling, and the other is a fast degradation of the structure within a short time [93,105–107]. For both situations, the structure reversibility is thought to be an essential factor. Based on some early studies on the in-situ XRD and the CV of LCO, the phase transitions would take place during (de)intercalation process. Two monoclinic phase transitions at about 50% and 80% lithium removal respectively lead to a structure shrink along the *c* axis of the LCO crystal, which are harmful to the structure reversibility of LCO and deteriorated to the performance of LCO based batteries. Therefore, the monoclinic phase transitions which would accelerate the capacity fading are expected to be avoided through modifications. In addition, there are other ways to improve the structural reversibility of materials. For example, Alcantara et al. [108] performed a careful study of B doped LCO provided better reversibility than bare LCO during the lithium (de)intercalation process which favored lattice adaptation to a superlattice structure of the lithium ions. Besides, structure stability and reversibility could also be improved via alteration of synthetic conditions that some reported Al-doped LCO presented better electrochemical reversibility than bare LCO [109–111].

Element doping is proved to be an effective way to improve structural stability/reversibility and alleviate capacity decay. Generally, element doping can improve capacity retention for prolonged cycles, but sacrifice the initial charge/discharge capacities due to the addition of non-active element [112]. Tukamoto et al. [71] first reported to improve the cycling performance of LCO at 4.3 V through Mg doping and proposed the mechanism of improved structure reversibility of LCO during the cycling process after doping. The enhanced stability was attributed to the occupation of Li vacancies by Mg ion, thus preventing the vacancy ordering. Therefore, the voltage plateau corresponding to the monoclinic phase transitions at around 4.2V was eliminated [113,114]. Fig. 6a–b shows the CV curve of $\text{LiCo}_{0.97}\text{Mg}_{0.03}\text{O}_2$ that the H2–M1 phase transition and the M1 to H3 phase transition at about 4.2V were suppressed after Mg doping, which referred as the improvement of structure reversibility [114]. To understand how did the doping suppresses the phase transition process would be a challenge. Dahn et al. [51] proposed the in-plane ordering configuration of lithium and vacancy during the H2 to M1 process based on the electrochemical and in situ XRD measurements of Li_xCoO_2 in 1992. Ceder et al. [53,115] approved the hypothesis through a first-principles study of the Li_xCoO_2 phase diagram, what's more, they reported the high mobility of the lithium vacancy may be the key reason of the first-order transition of LCO. Delmas et al. [58] also confirmed the lithium and vacancy ordering experimentally through electron diffraction investigations of a monoclinic $\text{Li}_{0.5}\text{CoO}_2$ sample which would reveal additional reflections. Despite all this, we were still uncertain about the disappearance of the monoclinic phase in some cases during the cycling process of LCO based LIBs.

When more and more lithium de-intercalated from LCO, more Co^{3+} is oxidized to Co^{4+} , which would lead to instability of the structure with high risks of the migration of Co^{4+} into Li^+ layers, due to the smaller size of Co^{4+} [19,21]. Besides, the local structural changes such as location and surrounding environment of Co^{4+} should also be taken into consideration since it would affect the cycling reversibility. A large number of vacancies in Li slab and a high concentration of Co^{4+} at HV would lead to the phase transition followed with a significant collapse of the crystal structure along the *c*-axis [2,26,27]. The LCO would accumulate lattice strain or even lead to mechanical failure on the extent contraction of the space lattice [95,116]. Therefore, strengthen the layer stability during cycling and decrease the stress accumulation are effective in the amelioration of the structure stability. Elemental doping will alleviate the deformation of the *c*-axis through physical routes, referred to as the pillaring effect. The doped elements in the lithium layer locate like pillars to decrease the collapse of crystal structure during cycling at HV, which can deteriorate the electrochemical performance of LCO. Kim

et al. [117] reported the improvement of electrochemical performance of LCO via Mg and Zr doping, they indicated that the Mg^{2+} and Zr^{4+} ions possessed the similar size to the Li^+ ions and they would locate at the inter-slab layer (Fig. 6c), thus they would not only provide a pathway for the (de)intercalation of lithium during the discharge/charge processes but also prevent the structure from distortion. Li et al. [118] partly substituted Li^+ by larger radius Na^+ to enlarge the Li slab and the lengths of Li–O was found reduced, which showed excellent HV and high-rate performance. Similar effects were reported on other cases of elemental doping including Ca^{2+} [119], Nb^{3+} [120], Zr^{4+} [121,122] in LCO. However, some doped elements such as Na^+ , which are also electrochemical active and can be removed from the inter-slab. Therefore, the stability of such materials during long cycle life applications is uncertain.

Whether surface modifications could affect the phase transitions of LCO has been under debate for a long time. Cho et al. [124–127] suggested the coating could stabilize the host structure of LCO and suppress the phase transitions of H2 to M1 of LCO, which were based on some cases of zero-stain materials. MgO-coated LCO cathode showed excellent cycle stability at 4.7 V, which was attributed to the phase transition at about 4.58 V is drastically suppressed due to the diffusion of Mg^{2+} from the MgO coating layer into the crystal [128,129]. Cao et al. [130] reported that the LiAlO_2 coated LCO showed a better cycling performance for the improvement of the structure reversibility of LCO in cycling. However, Dahn and some other researchers [128,131–135] argued that surface coating did not affect the phase transitions of LCO based on the in-situ XRD studies. Subsequent works were performed to study whether the coating would suppress the phase transitions of LCO. Liu et al. [132] found that the lattice parameters of Al_2O_3 coated LCO were similar to bare LCO after 50 cycles. The ALD coating of Al_2O_3 was also performed with the result that no change in phase transition would happen after coating [28]. What's more, the followed studies performed by them based on in situ XRD indicated distinctly that the variation range of the lattice parameters of Al_2O_3 coated LCO was much larger than bare LCO [136]. They also indicated that the coating would not suppress the phase transitions below 4.5 V, but would benefit to restrain the phase transition at about 4.58 V. Kalluri et al. [2] recently reported the $\text{LiNi}_{0.5}\text{Mn}_{0.5}\text{O}_2$ coated LCO went through smaller lattice volume changes during cycling based on the in-situ XRD survey. Therefore, it is still a lack of direct experimental evidence about the true function of surface coating on LCO. Surface coating could indirectly affect the bulk structural changes via two routes, one is to change the surface lithium content of LCO, the researches on lithium cobalt ratio studies [60,90] demonstrated the exceed lithium in bulk will suppress the order-disorder phase transition of LCO and it will appear with the removal of redundant lithium. The other is to spread into the subsurface or bulk to form a higher concentrated subsurface doping structure, several works also indicated the formation of doping during coating process because of the high temperature or a long-time thermal treatment [2,26,27,37,137]. Both of them would have significantly influence on the phase transition behavior of LCO in some respect [10–12].

3.2. Thermal stability

Thermal stability is important not only to the electrochemical performance but also to the safety of LIBs, which is always referred to as a major aspect of material modifications. Simultaneously, it is strongly corresponding to the stability of oxygen, the dissolution of transition metal and the irreversible phase transitions and even cracks of LCO during cycling or storage process. Studies on the aging mechanisms of LCO indicated that the failure in thermal stability is one of the most common modes, with strong relevance to the anodized oxide ions such as O^- or O species which have strong oxidation capabilities, the migration of cobalt, the phase transitions, and the accumulation of stress [104,138].

During the charging process, oxygen reactions are taking place at the

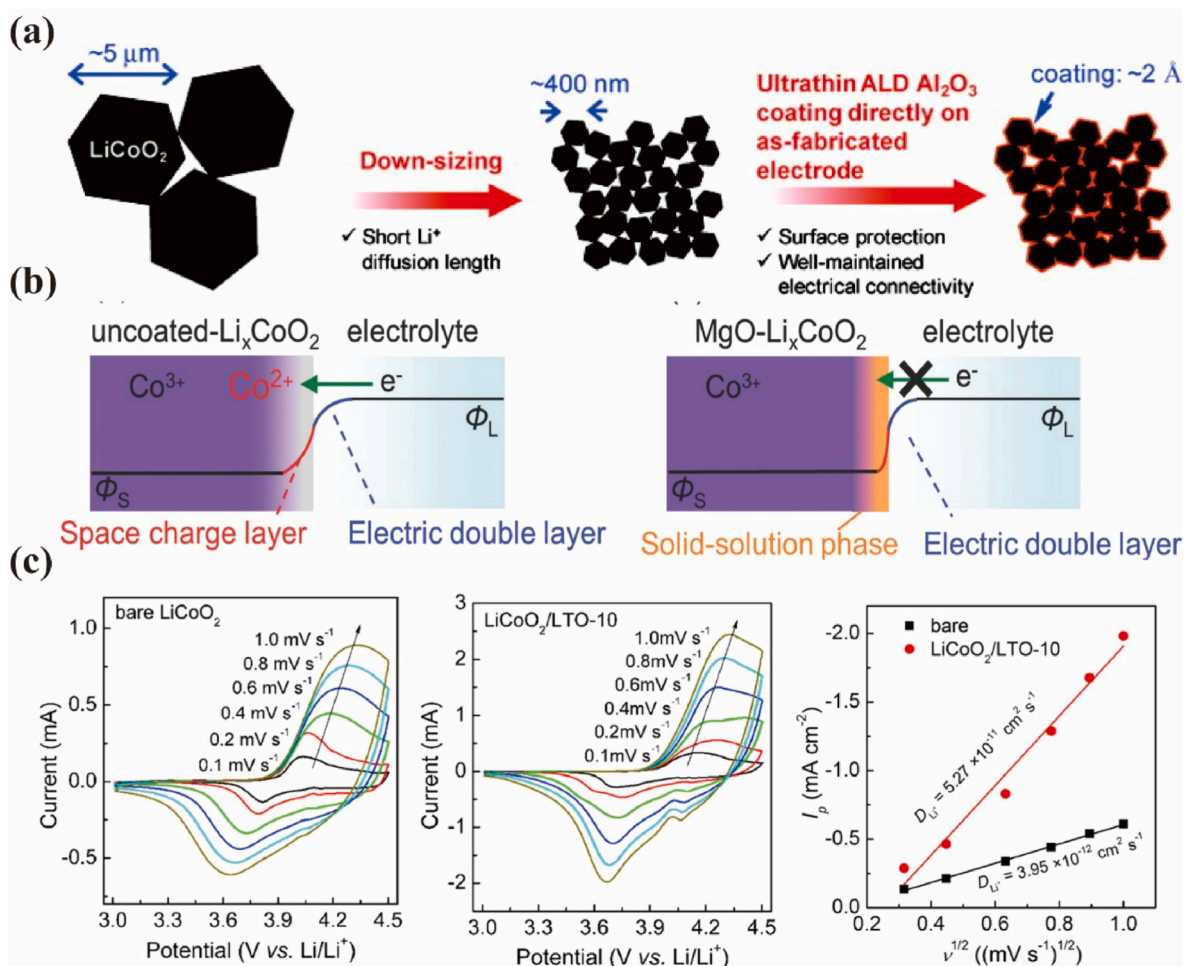


Fig. 7. a) Schematic view of modification mechanism through the ultrathin Al_2O_3 ALD coating [144]. (b) Schematic view of the electronic structure of uncoated and MgO-coated LCO/electrolyte interface upon electrolyte immersion (ϕ_S and ϕ_L are the electrochemical potentials of the electrode and electrolyte, respectively) [145]. (c) CV profiles of bare LiCoO_2 and $\text{LiCoO}_2/\text{Li}_4\text{Ti}_5\text{O}_{12}$ (LTO) with varying sweeping rates as well as the I_p - $v^{1/2}$ plots and the calculated D_{Li^+} [36].

cathode that the Co^{3+} was oxidized to Co^{4+} with a smaller radius and more active in reactivity. The cobalt atoms would be much easy to deviate from initial sites, along with the dissolution of cobalt metal as well as phase transitions. What's more, the phase transition would also be related to the stability of oxygen lattice. The oxygen anions such as O^{2-} , especially at HV, are possibly oxidized and become easier to migrate, leading to the formation of oxygen gas, with a rising of oxidation reactions with the electrolyte, the binder, etc. to speed up the fading of LIBs. In the meantime, huge stress would accumulate within the lattice of LCO particles, which can result in the formation and spreading of cracks. Therefore, the enhancement of thermal stability through modifications is essential to develop HV-LCO. Elemental doping can enhance the bulk thermal stability and surface coating will improve the surface thermal stability.

Hetero-metal doping such as Al, Mg, Ti is one of the most useful methods to enhance the bulk structural stability and possibly the bulk oxygen stability of LCO. Zou et al. [139] firstly reported the Mg-doped LCO, the $\text{LiMg}_{0.05}\text{Co}_{0.95}\text{O}_2$, cycled at 4.5 V with a discharge capacity of $\sim 160 \text{ mAh g}^{-1}$ at 0.2 C, and maintained capacity retention of 95% for more than 50 cycles. Similar doping elements such as Ca, Ba, etc. [119] were also reported to enhance the cycling electrochemical performance at HV. Dahn et al. compared the Al and Mg-doped LCO using accelerating rate calorimetry. The results indicated the superior performance of Al over Mg in enhancing the thermal stability of LCO [140]. Ti-doped LCO [141] is better in thermal safety than that of pristine LCO based on differential scanning calorimetry (DSC) measurement, further studies

disclosed the Ti-doped with a concentration gradient in LCO to form core-shell structure, therefore, Ti doping might improve the oxygen stability at near-surface.

Besides, some anions such as F^- were also reported to improve the electrochemical performance of LCO. Yonezawa et al. [142] reported the addition of LiF at the synthesis process of LCO would improve the cycling performance of LCO. Jung et al. [123] reported a metal and F co-doping method which could improve the thermal stability of LCO (Fig. 6d) and the fluorine substitution can stabilize the surface of the cathode to suppress the Co dissolution (Fig. 6e). Accordingly, the co-substituted materials displayed improved cycling performance as compared to pristine LiCoO_2 (Fig. 6f). So far, fluorides have been widely applied in surface modification to enhance the thermal stability of LCO. It would be discussed in detail at the following section 3.3.

The high-temperature performance involves the thermal stability of the LCO-based materials, which is essential to the practical application of the materials in LIBs, such as high-temperature storage and cycling. Materials with better thermal stability would be better at high temperatures. Gu et al. [143] demonstrated a spinel interfacial coating layer $\text{LiCo}_x\text{Mn}_{2-x}\text{O}_4$ which was formed in situ, owned excellent 45 °C cycling stability.

The thermal stability involves the safety of LIBs and would be a more important aspect to improve. It greatly corresponds to the stability of oxygen lattice. The improvement methods were including to introduce non-transition metal ions or to substitute oxygen atoms with fluorine. Surface coating with thermal stable materials would also improve the

interface stability.

3.3. Interface stability

It is well acknowledged that the stability of the interface plays a significant role in achieving a stable cycle performance of LCO. Fundamentally, the decomposition of electrolytes is a major issue affecting the stability of the interface [127,146–148]. To mitigate and/or address these issues, surface-coating is considered to be an effective method that has been widely used [124,131,149]. For example, Al_2O_3 coated LCO exhibits superior cycle performance over pure LCO. This coating layer, which acts as a physical barrier exists at the interface, can help to suppress the decomposition of the solvents and cobalt dissolution [126,132,150–152]. Besides, Scott et al. [144] used nanosizing LCO and coupled with ultrathin Al_2O_3 coating layer (about 2.2 Å) achieved excellent cycle stability and rate capability simultaneously. This improvement is highly related to the shortened diffusion path of Li ions by nanosizing and the promotion of interfacial stability by the coating layer (Fig. 7a). MgO coated LCO also possessed superior performance for its physical protection [153,154]. The mechanisms of MgO coating was demonstrated in Fig. 7b [145]. The destructed space charge layer resulting from the potential difference at the electrode surface can be observed in the uncoated LiCoO_2 , which leads to the irreversible change of the Co oxidation state. In contrast, although potential differences still exist at the interface for MgO coated LCO, the Mg^{2+} -containing solid solution phase and the stronger Mg–O bond could stabilize the surface structure and compensate for the potential differences on the surface. The results suggested that proper control of the electronic structure and space charge layer at the electrode/electrolyte interface is crucial to improving the interface stability of lithium batteries.

Opponent results were reported that Al or Mg-based oxide coating

would not take effect on improving the structural stability and the capacity fading was still obvious during the cycling process. Coating with oxides on LCO should carefully regulate the synthetic conditions and the thickness of the coating layer. Besides, it was evidenced that irreversible reactions between the oxides and electrolytes would affect the overall performance of LIBs [28,155,156]. In addition, the poor electronic conductivity brings about by the excessive oxides coating layer would increase the interface impedance and thus depress the electrochemical performance of LCO. However, conventional coating methods always went through thermal treatment at the high-temperature process, which could form solid solutions via reactions between metal oxides and the surface of LCO particles. Shao et al. [157] reported a $\text{LiAlO}_2/\text{LiCo}_{1-x}\text{Al}_x\text{O}_2$ double-layer coating strategy to improve the cycling performance at a high cut-off voltage and high temperature. This enhancement was profited from multiple functions including the physical isolation of the LiAlO_2 layer to the direct contact of electrolyte and the electrochemical stability as well as the lithium-ion conductivity improvement of the $\text{LiCo}_{1-x}\text{Al}_x\text{O}_2$ layer. Therefore, it was hard to ensure the influence of metal oxide coating on the surface conductivity properties. More detailed experimental evidence was required to settle the disputes.

In conclusion, proper amount of metal oxides and well-controlled synthetic conditions are essential to create highly stable surface on coated LCO. However, the excessive oxides will increase interface impedance which will lead to sluggish kinetics of electrodes.

Metal fluoride coatings could be a better choice to prevent HF attack, which would provide the surface of LCO with better stabilities. Both the surface coated fluorides and the oxyfluorides formed via reactions would remarkably improve the stability and safety of electrodes for usage in LIBs [158]. Park et al. [28] adopted the ALD method to coat an ultrathin aluminum–tungsten–fluoride film on the surface of LCO to reduce surface reactions including Co dissolution and electrolyte

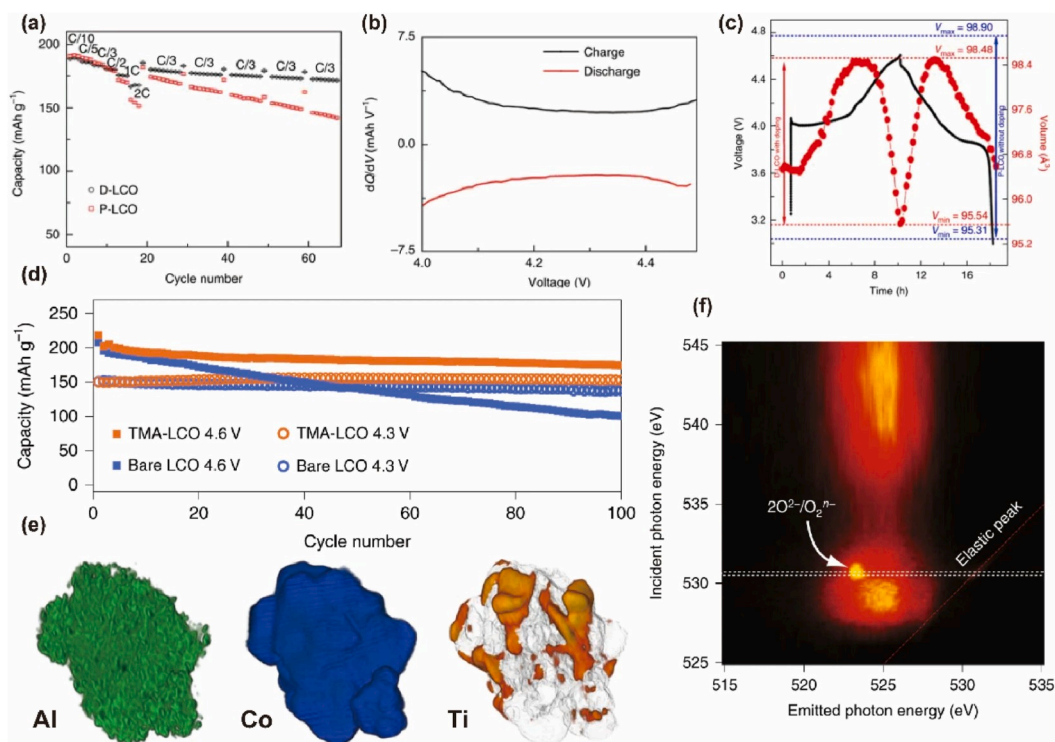


Fig. 8. (a–c) La–Al co-doped strategies achieved 4.5 V applications of LCO [77]. (a) Cycling performance comparison of P-LCO (pristine LiCoO_2) and D-LCO (La + Al co-doped LiCoO_2). (b) The dQ/dV curve of D-LCO during the formation test. (c) The voltage profile (black) and the cell volume evolution process (red) of doped-LCO. V_{max} and V_{min} are the maximum and minimum cell volume, respectively. The volume data are also shown (in blue) for pristine-LCO. (d–f) Ti–Mg–Al co-doped strategies (TMA-LCO) achieved 4.6 V applications of LCO [180]. (d) Comparison of cycle performances of LiCoO_2/Li half cells with bare LCO versus TMA-LCO. (e) 3D X-ray tomography reconstruction and element distribution in TMA-LCO. 3D spatial distributions of Al, Co, and Ti, probed by fluorescence-yield scanning transmission X-ray microscopy. (f) O K edge RIXS maps collected on 4.6 V charged bare LCO. (For interpretation of the references to colour in this figure legend, the reader is referred to the Web version of this article.)

oxidation. Zhou et al. [156] recently reported the AlF_3 atomic layer deposition on free-standing LCO electrodes to enhance the surface stability and to increase the working voltage. A systematic work reported by Sun et al. [159–161] discussed the mechanism of the AlF_3 coating layer, the results indicated that the AlF_3 would protect the LCO surface from the chemical attack of HF and to delay the followed phase transition to a spinel phase. Besides, the coating layer would reduce the formation of LiF films to decrease the interfacial impedance, which could be beneficial to stabilize the interface.

Surface modification with carbon-based materials and some polymers could enhance the electron conductivity and fast ion conductive materials would improve the lithium-ion conductivity [162]. Interface modification such as Al_2O_3 [126,163] and $\text{Li}_4\text{Ti}_5\text{O}_{12}$ [36] coating can provide better ionic diffusion property for LCO. Cho et al. [126] demonstrated that Al_2O_3 coating could perform better at higher rates. This is ascribed to the formation of $\text{LiCo}_{1-y}\text{Al}_y\text{O}_2$ solid solution on the surface which would enhance the ionic conductivity of LCO. Recently, Zhou et al. [36] reported a nanoscale $\text{Li}_4\text{Ti}_5\text{O}_{12}$ coating LCO that dramatically enhanced the rate capability with 113 mAh g^{-1} at 12 C, which is 70% larger than that of the uncoated LCO. This enhancement of rate performance is due to the great improvement of the Li^+ diffusion coefficient by an order of magnitude from 3.90×10^{-12} to $5.27 \times 10^{-11} \text{ cm}^2 \text{ s}^{-1}$ through the CV profiles (Fig. 7c). Park et al. [164] reported a surface modification strategy that coating the LCO with carbon black nano-layers, which boosted both lithium-ion and electronic conduction.

When the charging voltage is higher than 4.5V, nearly all of the available carbonate-based solvents could be oxidized and more Co^{4+} are formed, the surface of LCO would be more reactive and could react with the electrolyte seriously. Therefore, interface stability is extremely important to develop HV-LCO. In this respect, effective surface modifications with different compounds and extra electrolyte additives would be very useful.

Although some physical and chemical properties of LCO such as the ionic/electronic conductivity and the lithium (de)intercalation voltage would also be affected by modifications and make sense on the electrochemical performance of LCO. Ceder et al. [165] predicted that Al substitution would raise the Li (de)intercalation voltage using simulations. Then, they performed electrochemical tests of Al-substituted LCO and experimentally confirmed that both the working voltage and open-circuit voltage were increased [110,166]. Other elements including Mg [167], Ga [168], etc. were also discovered to enhance the intercalation voltage of LCO. Besides, the surface coating could provide similar effects. Xu et al. [169] indicated the surface coating with the high-voltage material would also improve the intercalation voltage over the nanometer scale based on calculated results. The electronic and ionic conductivity is closely related to the electrochemical performance, especially the rate capability of LCO-based cathode material. Substitution with some elements such as Li [75], Mg [71], Ga [170] could increase the electronic conductivity of LCO. In addition, the underlying mechanism is also investigated. Take Mg doping as an example. Tuka-moto et al. [71] found that with the increase of doping amounts, the electronic conductivity of LCO first decreases and follows by a sharp increase, which is two orders of magnitude higher than the pure LCO. This variation of electronic conductivity is highly relevant to the concentration of Co^{4+} , which is related to the amounts of electron holes. When the trace amounts (<0.04) of Mg are introduced, Mg^{2+} firstly occupies Li vacancies, leading to decrease valence of Co^{4+} . And thus, the conductivity is reduced due to the decrease of electron holes. However, With the increase of Mg^{2+} content (≥ 0.04), Mg^{2+} will occupy the Co sites and create Co^{4+} for the charge balance, which can produce more electron holes and thus enhance the electronic conductivity. However, adequate evidences were still lack to fully understand the effects. More studies were required in future to adjust such properties in modifications.

4. Progress and challenges in achieving 4.5 V + LCO materials

Even though LCO based materials have made great progress in the last 40 years, it is still far away from the growing demand for energy density. Improving the working voltage of LCO is an efficient method, but it suffers serious issues including the H1-3 phase transitions, the obvious evolution of oxygen gas, the serious interface degradation, etc. To achieve 4.5 V+ applications, the structure reversibility, the thermal stability, and the interface stability of LCO should all be taken into consideration to meet the requirements of cycling performance, energy density, and safety of LIBs. Therefore, multiple-modes modification methods are explored recently to match such harsh terms.

Liu et al. [77] developed a La and Al co-doping LCO that displayed an exceptionally high specific capacity of 190 mAh g^{-1} and excellent cycling stability of 96% capacity retention at the voltage range of 3–4.5V (Fig. 8a). The combination of dQ/dV and high energy-XRD characterizations proved that La and Al co-doping can stabilize the bulk structure by suppressing phase transition and alleviating volume change (Fig. 8b–c). Besides, with La and Al co-doping, the detrimental cracks on the surface are effectively mitigated. They proposed that the La atoms could act as pillars to increase the interlayer spacing and the Al atoms could suspend the H2 to an M1 phase transition during cycling. They provided us with a good method to take advantage of two doping elements to enhance the structural stability of LCO particles at HV. However, the H1-3 phase transition was not appeared according to the CV curves and the stability of the interface was not discussed in detail in this paper.

In pursuing a higher working voltage of LCO, many groups make extensive attempts in developing 4.6V LCO. Several years ago, Nithya et al. [174] demonstrated a co-doping method to synthesize a $\text{LiMg}_x\text{Cu}_y\text{Co}_{1-x-y}\text{O}_2$ cathode material, which delivered a specific capacity of about 200 mAh g^{-1} at 4.6 V and 0.2 C. The capacity retention was 88% after 100 cycles. They ascribed the excellent electrochemical performance to the synergistic effect of Mg and Cu doping. The introduction of Cu can enhance the conductivity and Mg substitution could stabilize the layered structure. It is well acknowledged that the interfacial stability is a critical factor that greatly affecting electrochemical performance. Recently, Qian et al. [37] showed ternary lithium, aluminum, fluorine-coated layer to hinder the direct contact with the electrolyte and reduce the dissolution of Co. Besides, the thin doping layer of Li–Al–Co–O–F solid solution formed on the subsurface can suppress the phase transition of LCO at HV of 4.55 V+. Despite this remarkable progress in developing HV LCO, the capacity and cycle stability are still unsatisfactory when using a single modification method.

In this regard, comprehensive modification strategies with a good combination of surface modification and bulk co-doping are required imperatively. Wang et al. reported a modification strategy based on common elements (Al, Mg, Ti) [175]. They enhanced the bulk, surface and grain boundaries stabilities, as well as ionic conductivity properties of materials to promote the HV performance of LCO at 4.6 V. Accordingly, Al + Mg bulk co-doping and surface Ti coating LCO, exhibits significantly improved cycle stability of 86% capacity retention over 100 cycles with high capacity of 174 mAh g^{-1} at 0.5C (Fig. 8d). In addition, multiscale and multifaceted characterizations are performed to provide us with intensive insights into the modification mechanisms. Zhang et al. [180] also proposed a modification method via trace Al–Mg–Ti co-doping to achieve great cyclability of LiCoO_2 at 4.6 V. 3D X-ray tomography reconstruction (Fig. 8e) and Resonant inelastic soft X-ray scattering (RIXS) maps (Fig. 8f) is performed to study the element distribution of particles and surface oxygen reaction respectively. Experimental results suggest that even trace Ti can't dope into the crystal lattice. Ti displays a large degree of segregation on the surface, which can help to stabilize the surface microstructure and suppress the oxygen redox. Furthermore, density functional theory also proves that Ti doping can help to reduce the charge deficiency of the O atoms during the deep de-lithiation process to inhibit surface oxygen reaction. In recent work,

Hu et al. [181] performed isotope labeling ^{17}O NMR of LCO at the different charge of state to study the evolution of local oxygen environments. A clear variation of chemical shift and peak shape is observed in the ^{17}O NMR spectrum after deep de-lithiation. If combining nuclear magnetic calculation and other characterization such as RIXS in the future, a more in-depth and comprehensive understanding of the LCO structure even atomic-level can be obtained.

In addition to these modifications and characterizations on the LCO, many works focus on the optimization of additives in the electrolyte to develop HV LIBs [178,179,182,183]. Electrolyte additive is a more simple and cost-efficient method to stabilize the interface, suppress electrolyte degradation and cobalt dissolution and thus improve the high-voltage performance. For example, Li et al. [183] reported the cyclability enhancement strategies via adding vinyl ethylene carbonate (VEC) in the electrolyte. $\text{LiCoO}_2/\text{graphite}$ pouch cells using this additive exhibit excellent cycle performance of 88% capacity retention over 400 cycles from 3 to 4.5V at 1C. They proposed that the VEC additive could form both CEI and SEI films to cover the active sites and thus suppress electrolyte decomposition and Co dissolution. In addition, other aspects like solvents, lithium salt should also be optimized and modified so that the electrolyte can adapt to challenges of high voltage. Except for electrolyte additives, utilization of solid-state electrolytes with wide electrochemical window can be a good choice to mitigate electrolyte oxidative decomposition induced by high-voltage, thereby improving electrolyte stability. Some non-electrochemical parts including the separator, the binders, and conductive carbon, etc. also play a critical role in LIBs. However, these parts always suffer from challenges at a higher voltage but lack of comprehensive research for modifying them. Zhang et al. [184] demonstrated that the separator would shrink quickly over softening temperature and the basic requirement of the shrinkage should less than 5% after 60 min at 90 °C for LIBs. Besides, LCO-based LIBs will release more heat and occur more complex electrochemical reactions at high-voltage (4.5V+), leading to the poor thermal shrinkage property and even the destroyed ionic conductivity. Besides, the binder should be electrochemically inertness and simultaneously provide enough adhesion to bear the giant volume change. Whereas, these properties of binders exhibit a big discount at higher voltage so that it no longer affords satisfactory performance. Accordingly, to achieve high-voltage LCO-based LIBs, a synthetic survey of battery system including the non-electrochemical parts should be all taken into consideration and amelioration.

Currently, the most popular commercial LIBs are the LCO/graphite system. To further improve the energy density of LIBs, the other novel battery systems are reported. For instance, Li metal anodes could improve the energy density of LIBs. However, Li metal anodes are not primed to commercial applications owing to the safety problems. Silicon-based materials are promising for their ultra-high theoretical capacity and abundant storage in the earth, however, disadvantages such as huge volume change during charge/discharge also limit their further applications [40].

The intensified problems at high voltage (4.5V+), including instability of the bulk, surface, and interface, will greatly damage the electrochemical performance and increase the safety risk. In addition, the energy density of LCO has gradually approached the upper limit. Therefore, the prospective applications of the LCO based cathode materials should seek for new ways in varieties of LIBs systems. We anticipate that the solid-state batteries should be a suitable choice for HV-LCO for its advantages of high safety and high energy density [185]. Nonetheless, the conductivity, as well as the interface compatibility between the LCO and the solid electrolyte, remains arduous challenges to limit their applications.

5. Conclusion and perspective

After 40 years' discovery of LiCoO_2 as a reversible 4V cathode for Li-ion battery, nearly 0.7 Li in LiCoO_2 can be reversibly utilized ($\sim 195\text{mAh}$

g^{-1}) in most advanced Li-ion batteries. Can we utilize more reversible Li ions in the future generation of Li-ion battery? What is the practical upper limit of useable Li-ions and a working voltage of a layered LCO? These questions have to be carefully investigated and call for further understanding. Besides, the real working mechanism of different doping elements should be quantitatively evaluated. The interfacial modification strategy of LCO is practically useful, but it usually requires advanced functional electrolytes to form stable cathode electrolyte interfaces (CEI). Apparently, the design of stable CEI on LCO by novel additives and molecular-assembling in future calls for more precise control and quantitative characterization with the help of advanced spectroscopic techniques. Certainly, some important directions for future application of high energy density LIBs cannot be ignored. The first one is that more and more solid-state electrolytes will be used in practical Li-ion battery, either used as coating materials for LCO or to increase the ionic conductivity of the electrolytes with less organic solvents. The second one is the utilization of other new developed layered cathode materials, such as Ni-riched NCM to instead of LCO for some specific applications. In addition, the transformation of the graphite-based anode to Si-containing or Li-containing anode will become the main developing trend. Anyway, LCO will slowly approach its theoretical capacity or working voltage limit. However, how to acquire higher energy density or even approaching its theoretical capacity and make it realize more stable, cheaper and safer electrodes and corresponding batteries still has some ways to go.

Declaration of competing interest

The authors declare that they have no known competing financial interests or personal relationships that could have appeared to influence the work reported in this paper.

Acknowledgment

This work is financially supported by the National Natural Science Foundation of China (Grant no. 21761132030, 21935009) and Cooperative Project of Production and Study at the University of Fujian Province (2018H6020).

References

- [1] T. Nagaura, *Progress Batter. Solar Cells* 9 (1990) 209.
- [2] S. Kalluri, M. Yoon, M. Jo, S. Park, S. Myeong, J. Kim, S.X. Dou, Z. Guo, J. Cho, *Adv. Energy Mater.* 7 (2017) 1601507.
- [3] J.M. Tarascon, M. Armand, *Nature* 414 (2001) 359–367.
- [4] M. Armand, J.M. Tarascon, *Nature* 451 (2008) 652.
- [5] T. Ohzuku, A. Ueda, M. Nagayama, Y. Iwakoshi, H. Komori, *Electrochim. Acta* 38 (1993) 1159–1167.
- [6] Y. Nishi, *J. Power Sources* 100 (2001) 101–106.
- [7] E. Antolini, *Solid State Ionics* 170 (2004) 159–171.
- [8] M. Li, J. Lu, Z. Chen, K. Amine, *Adv. Mater.* 30 (2018) 1800561.
- [9] K. Mizushima, P.C. Jones, P.J. Wiseman, J.B. Goodenough, *Mater. Res. Bull.* 15 (1980) 783–789.
- [10] Z. Tian, H. Yu, Z. Zhang, X. Xu, *ChemBioEng Rev.* 5 (2018) 111–118.
- [11] J.W. Fergus, *J. Power Sources* 195 (2010) 939–954.
- [12] L. Wang, B. Chen, J. Ma, G. Cui, L. Chen, *Chem. Soc. Rev.* 47 (2018) 6505–6602.
- [13] M. Winter, B. Barnett, K. Xu, *Chem. Rev.* 118 (2018) 11433–11456.
- [14] J. Wu, P. Lin, Y. Hu, H. Li, *Energy Storage Sci. Technol.* 5 (2016) 443–453.
- [15] W. Li, B. Song, A. Manthiram, *Chem. Soc. Rev.* 46 (2017) 3006–3059.
- [16] M.R. Palacin, *Chem. Soc. Rev.* 38 (2009) 2565–2575.
- [17] G.G. Amatucci, J.M. Tarascon, L.C. Klein, *J. Electrochem. Soc.* 143 (1996) 1114–1123.
- [18] A. Zhou, Q. Liu, Y. Wang, W. Wang, X. Yao, W. Hu, L. Zhang, X. Yu, J. Li, H. Li, *J. Mater. Chem.* 5 (2017) 24361–24370.
- [19] G.G. Amatucci, J.M. Tarascon, L.C. Klein, *Solid State Ionics* 83 (1996) 167–173.
- [20] Z. Chen, J.R. Dahn, *Electrochim. Acta* 49 (2004) 1079–1090.
- [21] A.J. Smith, H.M. Dahn, J.C. Burns, J.R. Dahn, *J. Electrochem. Soc.* 159 (2012) A705–A710.
- [22] P. He, H. Yu, D. Li, H. Zhou, *J. Mater. Chem.* 22 (2012) 3680.
- [23] M. Park, X. Zhang, M. Chung, G.B. Less, A.M. Sastry, *J. Power Sources* 195 (2010) 7904–7929.
- [24] Z. Chen, Z. Lu, J. Dahn, *J. Electrochem. Soc.* 149 (2002) A1604–A1609.
- [25] G.T.-K. Fey, T.P. Kumar, *J. Ind. Eng. Chem.* 10 (2004) 1090–1103.

- [26] H. Li, Z. Wang, L. Chen, X. Huang, *Adv. Mater.* 21 (2009) 4593–4607.
- [27] C. Li, H.P. Zhang, L.J. Fu, H. Liu, Y.P. Wu, E. Rahm, R. Holze, H.Q. Wu, *Electrochim. Acta* 51 (2006) 3872–3883.
- [28] J.S. Park, A.U. Mane, J.W. Elam, J.R. Croy, *Chem. Mater.* 27 (2015) 1917–1920.
- [29] B.C. Melot, J.M. Tarascon, *Acc. Chem. Res.* 46 (2013) 1226–1238.
- [30] G. Crabtree, E. Kócs, L. Trahey, *MRS Bull.* 40 (2015) 1067–1078.
- [31] E.J. Berg, C. Villavieille, D. Streich, S. Trabesinger, P. Novák, *J. Electrochem. Soc.* 162 (2015) A2468–A2475.
- [32] S.B. Chikkannanavar, D.M. Bernardi, L. Liu, *J. Power Sources* 248 (2014) 91–100.
- [33] K. Xu, *Chem. Rev.* 114 (2014) 11503–11618.
- [34] A. Aboulaich, K. Ouzaoui, H. Faqir, A. Kaddami, I. Benzakour, I. Akalay, *Mater. Res. Bull.* 73 (2016) 362–368.
- [35] S. Kim, C. Kim, Y.-I. Jhon, J.-K. Noh, S.H. Vemuri, R. Smith, K.Y. Chung, M. S. Jhon, B.-W. Cho, *J. Mater. Chem.* 22 (2012) 25418–25426.
- [36] A. Zhou, X. Dai, Y. Lu, Q. Wang, M. Fu, J. Li, *ACS Appl. Mater. Interfaces* 8 (2016) 34123–34131.
- [37] J. Qian, L. Liu, J. Yang, S. Li, X. Wang, H.L. Zhuang, Y. Lu, *Nat. Commun.* 9 (2018) 4918.
- [38] N.-S. Choi, J.-G. Han, S.-Y. Ha, I. Park, C.-K. Back, *RSC Adv.* 5 (2015) 2732–2748.
- [39] A.M. Tripathi, W.-N. Su, B.J. Hwang, *Chem. Soc. Rev.* 47 (2018) 736–851.
- [40] J. Liu, Z. Bao, Y. Cui, E.J. Dufek, J.B. Goodenough, P. Khalifah, Q. Li, B.Y. Liaw, P. Liu, A. Manthiram, Y.S. Meng, V.R. Subramanian, M.F. Toney, V. Viswanathan, M.S. Whittingham, J. Xiao, W. Xu, J. Yang, X.-Q. Yang, J.-G. Zhang, *Nat. Energy* 4 (2019) 180–186.
- [41] L. Xia, Y.-G. Xia, Z.-P. Liu, *Electrochimica Acta* 151 (2015) 429–436.
- [42] T. Ohzuku, Y. Makimura, *Chem. Lett.* 30 (2001) 744–745.
- [43] T. Ohzuku, Y. Makimura, *Chem. Lett.* 30 (2001) 642–643.
- [44] Y.-K. Lin, C.-H. Lu, H.-C. Wu, M.-H. Yang, *J. Power Sources* 146 (2005) 594–597.
- [45] M. Bianchini, M. Roca-Ayats, P. Hartmann, T. Brezesinski, J. Janek, *Angew. Chem. Int. Ed.* 58 (2019) 10434–10458.
- [46] A. Mauger, C.M. Julien, J.B. Goodenough, K. Zaghib, *J. Electrochem. Soc.* 167 (2020), 070507.
- [47] C. Delmas, J.-J. Braconnier, P. Hagemuller, *Mater. Res. Bull.* 17 (1982) 117–123.
- [48] D. Carlier, I. Saadoun, M. Ménétrier, C. Delmas, *J. Electrochem. Soc.* 149 (2002) A1310–A1320.
- [49] Y. Shao-Horn, F. Weill, L. Croguennec, D. Carlier, M. Ménétrier, C. Delmas, *Chem. Mater.* 15 (2003) 2977–2983.
- [50] R. Siegel, J. Hirschinger, D. Carlier, S. Matar, M. Ménétrier, C. Delmas, *J. Phys. Chem. B* 105 (2001) 4166–4174.
- [51] J.N. Reimers, J.R. Dahn, *J. Electrochem. Soc.* 139 (1992) 2091–2097.
- [52] T. Ohzuku, A. Ueda, *J. Electrochem. Soc.* 141 (1994) 2972–2977.
- [53] A. Van der Ven, M.K. Aydinol, G. Ceder, J. Hafner, *Phys. Rev. B* 58 (1998) 2975–2987.
- [54] X. Lu, Y. Sun, Z. Jian, X. He, L. Gu, Y.-S. Hu, H. Li, Z. Wang, W. Chen, X. Duan, L. Chen, J. Maier, S. Tsukimoto, Y. Ikuhara, *Nano Lett.* 12 (2012) 6192–6197.
- [55] E. Plichta, S. Slane, M. Uchiyama, M. Salomon, D. Chua, W.B. Ebner, H.W. Lin, *J. Electrochem. Soc.* 136 (1989) 1865–1869.
- [56] M. Ménétrier, I. Saadoun, S. Levasseur, C. Delmas, *J. Mater. Chem.* 9 (1999) 1135–1140.
- [57] C. Wolverton, A. Zunger, *Phys. Rev. Lett.* 81 (1998) 606–609.
- [58] Y. Shao-Horn, S. Levasseur, F. Weill, C. Delmas, *J. Electrochem. Soc.* 150 (2003) A366–A373.
- [59] S. Levasseur, M. Ménétrier, Y. Shao-Horn, L. Gautier, A. Audemer, G. Demazeau, A. Largeteau, C. Delmas, *Chem. Mater.* 15 (2003) 348–354.
- [60] S. Levasseur, M. Ménétrier, E. Suard, C. Delmas, *Solid State Ionics* 128 (2000) 11–24.
- [61] A. Van der Ven, M.K. Aydinol, G. Ceder, *J. Electrochem. Soc.* 145 (1998) 2149–2155.
- [62] Y.S. Meng, M.E. Arroyo-de Dompablo, *Acc. Chem. Res.* 46 (2013) 1171–1180.
- [63] H. Gabrisch, R. Yazami, B. Fultz, *Electrochim. Solid State Lett.* 5 (2002) A111–A114.
- [64] Y. Takahashi, Y. Gotoh, J. Akimoto, S. Mizuta, K. Tokiwa, T. Watanabe, *J. Solid State Chem.* 164 (2002) 1–4.
- [65] K. Dokko, M. Mohamedi, Y. Fujita, T. Itoh, M. Nishizawa, M. Umeda, I. Uchida, *J. Electrochem. Soc.* 148 (2001) A422–A426.
- [66] T. Bak, J. Nowotny, M. Rekas, C.C. Sorrell, S. Sugihara, *Ionics* 6 (2000) 92–106.
- [67] M. Shibuya, T. Nishina, T. Matsue, I. Uchida, *J. Electrochem. Soc.* 143 (1996) 3157–3160.
- [68] A. Van der Ven, G. Ceder, *Electrochim. Solid State Lett.* 3 (2000) 301–304.
- [69] A. Van der Ven, G. Ceder, *J. Power Sources* 97–98 (2001) 529–531.
- [70] J. van Elp, J.L. Wieland, H. Eskes, P. Kuiper, G.A. Sawatzky, F.M.F. de Groot, T. S. Turner, *Phys. Rev. B* 44 (1991) 6090–6103.
- [71] H. Tukamoto, A.R. West, *J. Electrochem. Soc.* 144 (1997) 3164–3168.
- [72] K.M. Abraham, D.M. Pasquariello, E.M. Willstaedt, *J. Electrochem. Soc.* 145 (1998) 482–486.
- [73] J. Wolfenstine, *J. Power Sources* 129 (2004) 324–325.
- [74] J. Molenda, A. Stoklosa, T. Bgk, *Solid State Ionics* 36 (1989) 53–58.
- [75] M. Carewska, S. Scaccia, F. Croce, S. Arumugam, Y. Wang, S. Greenbaum, *Solid State Ionics* 93 (1997) 227–237.
- [76] J. Barker, R. Pynenburg, R. Koksang, M.Y. Saidi, *Electrochim. Acta* 41 (1996) 2481–2488.
- [77] Q. Liu, X. Su, D. Lei, Y. Qin, J. Wen, F. Guo, Y.A. Wu, Y. Rong, R. Kou, X. Xiao, F. Aguesse, J. Bareño, Y. Ren, W. Lu, Y. Li, *Nat. Energy* 3 (2018) 936–943.
- [78] V.R. Galakhov, E.Z. Kurmaev, S. Uhlenbrock, M. Neumann, D.G. Kellerman, V. S. Gorskikh, *Solid State Commun.* 99 (1996) 221–224.
- [79] M. Tabuchi, K. Ado, H. Kobayashi, H. Sakaabe, H. Kageyama, C. Masquelier, M. Yonemura, A. Hirano, R. Kanno, *J. Mater. Chem.* 9 (1999) 199–204.
- [80] V.L. McLaren, A.R. West, M. Tabuchi, A. Nakashima, H. Takahara, H. Kobayashi, H. Sakaabe, H. Kageyama, A. Hirano, Y. Takeda, *J. Electrochem. Soc.* 151 (2004) A672–A681.
- [81] F.M.F. de Groot, M. Abbate, J. van Elp, G.A. Sawatzky, Y.J. Ma, C.T. Chen, F. Sette, *J. Phys. Condens. Matter* 5 (1993) 2277–2288.
- [82] L.A. Montoro, M. Abbate, J.M. Rosolen, *Electrochim. Solid State Lett.* 3 (2000) 410–412.
- [83] Y. Uchimoto, H. Sawada, T. Yao, *J. Synchrotron Radiat.* 8 (2001) 872–873.
- [84] N.V. Kosova, V.V. Kaichev, V.I. Bukhtiyarov, D.G. Kellerman, E.T. Devyatkina, T. V. Larina, *J. Power Sources* 119–121 (2003) 669–673.
- [85] L. Dahéron, R. Dedryvère, H. Martinez, M. Ménétrier, C. Denage, C. Delmas, D. Gonbeau, *Chem. Mater.* 20 (2008) 583–590.
- [86] S. Gopukumar, Y. Jeong, K.B. Kim, *Solid State Ionics* 159 (2003) 223–232.
- [87] W.S. Yoon, K.K. Lee, K.B. Kim, *J. Electrochem. Soc.* 147 (2000) 2023–2028.
- [88] W.-S. Yoon, K.-B. Kim, M.-G. Kim, M.-K. Lee, H.-J. Shin, J.-M. Lee, *J. Electrochem. Soc.* 149 (2002) A1305–A1309.
- [89] C. Julien, *Solid State Ionics* 157 (2003) 57–71.
- [90] S. Levasseur, M. Ménétrier, C. Delmas, *Chem. Mater.* 14 (2002) 3584–3590.
- [91] M. Peeters, M. Van Bommel, H. Van Hal, W. Keur, A.P.M. Kentgens, *Solid State Ionics* 112 (1998) 41–52.
- [92] M. Murakami, Y. Noda, Y. Koyama, K. Takegoshi, H. Arai, Y. Uchimoto, Z. Ogumi, *J. Phys. Chem. C* 118 (2014) 15375–15385.
- [93] D. Aurbach, B. Markovsky, A. Rodkin, M. Cojocaru, E. Levi, H.-J. Kim, *Electrochim. Acta* 47 (2002) 1899–1911.
- [94] D. Aurbach, B. Markovsky, A. Rodkin, E. Levi, Y. Cohen, H.-J. Kim, M. Schmidt, *Electrochim. Acta* 47 (2002) 4291–4306.
- [95] D. Zhang, B.S. Haran, A. Durairajan, R.E. White, Y. Podrazhansky, B.N. Popov, *J. Power Sources* 91 (2000) 122–129.
- [96] J. Fan, P.S. Fedkiw, *J. Power Sources* 72 (1998) 165–173.
- [97] G. Ning, B. Haran, B.N. Popov, *J. Power Sources* 117 (2003) 160–169.
- [98] R. Fathi, J.C. Burns, D.A. Stevens, H. Ye, C. Hu, G. Jain, E. Scott, C. Schmidt, J. R. Dahn, *J. Electrochem. Soc.* 161 (2014) A1572–A1579.
- [99] Z. Chen, J.R. Dahn, *Electrochim. Solid State Lett.* 7 (2004) A11–A14.
- [100] P. Ramadass, B. Haran, R. White, B.N. Popov, *J. Power Sources* 112 (2002) 614–620.
- [101] H. Wang, Y.-I. Jang, B. Huang, D.R. Sadoway, Y.-M. Chiang, *J. Power Sources* 81–82 (1999) 594–598.
- [102] H. Wang, Y.-I. Jang, B. Huang, D.R. Sadoway, Y.-M. Chiang, *J. Electrochem. Soc.* 146 (1999) 473–480.
- [103] R. Yazami, Y. Ozawa, H. Gabrisch, B. Fultz, *Electrochim. Acta* 50 (2004) 385–390.
- [104] J. Vetter, P. Novák, M.R. Wagner, C. Veit, K.C. Möller, J.O. Besenhard, M. Winter, M. Wohlfahrt-Mehrens, C. Vogler, A. Hammouche, *J. Power Sources* 147 (2005) 269–281.
- [105] M. Gauthier, T.J. Carney, A. Grimaud, L. Giordano, N. Pour, H.-H. Chang, D. P. Fenning, S.F. Lux, O. Paschos, C. Bauer, F. Maglia, S. Lupart, P. Lamp, Y. Shao-Horn, *J. Phys. Chem. Lett.* 6 (2015) 4653–4672.
- [106] M. Broussely, P. Biensan, F. Bonhomme, P. Blanchard, S. Herreyre, K. Nechev, R. J. Staniewicz, *J. Power Sources* 146 (2005) 90–96.
- [107] M. Wohlfahrt-Mehrens, C. Vogler, J. Garche, *J. Power Sources* 127 (2004) 58–64.
- [108] R. Alcántara, P. Lavela, J.L. Tirado, R. Stoyanova, E. Zhecheva, *J. Solid State Chem.* 134 (1997) 265–273.
- [109] N. Amdouni, H. Zarrouk, F. Soulette, C. Julien, *Mater. Chem. Phys.* 80 (2003) 205–214.
- [110] S.-T. Myung, N. Kumagai, S. Komaba, H.-T. Chung, *Solid State Ionics* 139 (2001) 47–56.
- [111] W.-S. Yoon, K.-K. Lee, K.-B. Kim, *Electrochim. Solid State Lett.* 4 (2001) A35–A37.
- [112] S. Castro-Garcia, A. Castro-Couceiro, M.A. Senaris-Rodriguez, F. Soulette, C. Julien, *Solid State Ionics* 156 (2003) 15–26.
- [113] M.V. Reddy, T.W. Jie, C.J. Jafta, K.I. Ozoemena, M.K. Mathe, A.S. Nair, S.S. Peng, M.S. Idris, G. Balakrishna, F.I. Ezema, B.V.R. Chowdari, *Electrochim. Acta* 128 (2014) 192–197.
- [114] X. Zhu, K. Shang, X. Jiang, X. Ai, H. Yang, Y. Cao, *Ceram. Int.* 40 (2014) 11245–11249.
- [115] C.A. Marianetti, G. Kotliar, G. Ceder, *Nat. Mater.* 3 (2004) 627–631.
- [116] A. Yano, M. Shikano, A. Ueda, H. Sakaabe, Z. Ogumi, *J. Electrochem. Soc.* 164 (2017) A6116–A6122.
- [117] H.-S. Kim, T.-K. Ko, B.-K. Na, W.I. Cho, B.W. Chao, *J. Power Sources* 138 (2004) 232–239.
- [118] Q. Li, K. Wu, M. Chen, Y.L. Lee, D. Chen, M. Wu, F. Li, X. Xiao, Z. Hu, *Electrochim. Acta* 273 (2018) 145–153.
- [119] R. Sathiyamoorthi, R. Chandrasekaran, A. Gopalan, T. Vasudevan, *Mater. Res. Bull.* 43 (2008) 1401–1411.
- [120] K. Wu, Q. Li, M. Chen, D. Chen, M. Wu, Z. Hu, F. Li, X. Xiao, *J. Solid State Electrochem.* 22 (2018) 3725–3734.
- [121] F. Nobili, F. Croce, R. Tossici, I. Meschini, P. Reale, R. Marassi, *J. Power Sources* 197 (2012) 276–284.
- [122] M. Zou, M. Yoshio, S. Gopukumar, J.-i. Yamaki, *Chem. Mater.* 17 (2005) 1284–1286.
- [123] H.-G. Jung, N.V. Gopal, J. Prakash, D.-W. Kim, Y.-K. Sun, *Electrochim. Acta* 68 (2012) 153–157.
- [124] J. Cho, Y.J. Kim, T.-J. Kim, B. Park, *Angew. Chem. Int. Ed. Engl.* 40 (2001) 3367–3369.
- [125] J. Cho, Y.J. Kim, B. Park, *J. Electrochem. Soc.* 148 (2001) A1110–A1115.

- [126] J. Cho, Y.J. Kim, B. Park, *Chem. Mater.* 12 (2000) 3788–3791.
- [127] Y.J. Kim, J. Cho, T.-J. Kim, B. Park, *J. Electrochem. Soc.* 150 (2003) A1723–A1725.
- [128] Z. Wang, L. Liu, L. Chen, X. Huang, *Solid State Ionics* 148 (2002) 335–342.
- [129] Z. Wang, C. Wu, L. Liu, F. Wu, L. Chen, X. Huang, *J. Electrochem. Soc.* 149 (2002) A466–A471.
- [130] H. Cao, B. Xia, Y. Zhang, N. Xu, *Solid State Ionics* 176 (2005) 911–914.
- [131] Z. Chen, J.R. Dahn, *Electrochem. Solid State Lett.* 5 (2002) A213–A216.
- [132] L. Liu, Z. Wang, H. Li, L. Chen, X. Huang, *Solid State Ionics* 152–153 (2002) 341–346.
- [133] Z. Chen, J.R. Dahn, *Electrochem. Solid State Lett.* 6 (2003) A221–A224.
- [134] N.V. Kosova, E.T. Devyatkina, *J. Power Sources* 174 (2007) 959–964.
- [135] Y.S. Jung, A.S. Cavanagh, A.C. Dillon, M.D. Groner, S.M. George, S.-H. Lee, *J. Electrochem. Soc.* 157 (2010) A75–A81.
- [136] L. Liu, L. Chen, X. Huang, X.-Q. Yang, W.-S. Yoon, H. Lee, J. McBreen, *J. Electrochem. Soc.* 151 (2004) A1344–A1351.
- [137] J. Cho, G. Kim, *Electrochem. Solid State Lett.* 2 (1999) 253–255.
- [138] S. Sharifi-Asl, F.A. Soto, A. Nie, Y. Yuan, H. Asayesh-Ardakani, T. Foroozan, V. Yurkiv, B. Song, F. Mashayek, R.F. Klie, K. Amine, J. Lu, P.B. Balbuena, R. Shahbazian-Yassar, *Nano Lett.* 17 (2017) 2165–2171.
- [139] M. Zou, M. Yoshio, S. Gopukumar, J.-i. Yamaki, *Electrochem. Solid State Lett.* 7 (2004) A176.
- [140] F. Zhou, W. Luo, X. Zhao, J.R. Dahn, *J. Electrochem. Soc.* 156 (2009) A917–A920.
- [141] J. Yu, Z. Han, X. Hu, H. Zhan, Y. Zhou, X. Liu, *J. Power Sources* 225 (2013) 34–39.
- [142] S. Yonezawa, T. Okayama, H. Tsuda, M. Takashima, *J. Fluor. Chem.* 87 (1998) 141–143.
- [143] R. Gu, Z. Ma, T. Cheng, Y. Lyu, A. Nie, B. Guo, *ACS Appl. Mater. Interfaces* 10 (2018) 31271–31279.
- [144] I.D. Scott, Y.S. Jung, A.S. Cavanagh, Y. Yan, A.C. Dillon, S.M. George, S.-H. Lee, *Nano Lett.* 11 (2011) 414–418.
- [145] Y. Orikasa, D. Takamatsu, K. Yamamoto, Y. Koyama, S. Mori, T. Masese, T. Mori, T. Minato, H. Tanida, T. Uruga, Z. Ogumi, Y. Uchimoto, *Adv. Mater. Interfaces* 1 (2014) 1400195.
- [146] H. Lee, M.G. Kim, J. Cho, *Electrochem. Commun.* 9 (2007) 149–154.
- [147] G.-r. Hu, J.-c. Cao, Z.-d. Peng, Y.-b. Cao, K. Du, *Electrochim. Acta* 149 (2014) 49–55.
- [148] E. Endo, T. Yasuda, A. Kita, K. Yamaura, K. Sekai, *J. Electrochem. Soc.* 147 (2000) 1291–1294.
- [149] A.M. Kannan, L. Rabenberg, A. Manthiram, *Electrochem. Solid State Lett.* 6 (2003) A16–A18.
- [150] S. Sheng, G. Chen, B. Hu, R. Yang, Y. Xu, *J. Electroanal. Chem.* 795 (2017) 59–67.
- [151] H.J. Kwon, D.G. Park, *Electrochem. Solid State Lett.* 3 (2000) 128–130.
- [152] J. Cho, C.S. Kim, S.I. Yoo, *Electrochem. Solid State Lett.* 3 (2000) 362–365.
- [153] M. Mladenov, R. Stoyanova, E. Zhecheva, S. Vassilev, *Electrochem. Commun.* 3 (2001) 410–416.
- [154] Z. Wang, X. Huang, L. Chen, *J. Electrochem. Soc.* 150 (2003) A199–A208.
- [155] W.-D. Yang, C.-Y. Hsieh, H.-J. Chuang, Y.-S. Chen, *Ceram. Int.* 36 (2010) 135–140.
- [156] Y. Zhou, Y. Lee, H. Sun, J.M. Wallas, S.M. George, M. Xie, *ACS Appl. Mater. Interfaces* 9 (2017) 9614–9619.
- [157] L. Shao, L. Zhou, L. Yang, C. Jia, C. Wang, S. Hu, X. Zeng, C. Yang, C. Huang, Y. Zhou, X. Xi, *Electrochim. Acta* 297 (2019) 742–748.
- [158] G.G. Amatucci, N. Pereira, J. Fluor. Chem. 128 (2007) 243–262.
- [159] Y.-K. Sun, C.S. Yoon, S.-T. Myung, I. Belharouak, K. Amine, *J. Electrochem. Soc.* 156 (2009) A1005–A1010.
- [160] Y.K. Sun, S.W. Cho, S.T. Myung, K. Amine, J. Prakash, *Electrochim. Acta* 53 (2007) 1013–1019.
- [161] Y. Sun, J. Han, S. Myung, S. Lee, K. Amine, *Electrochem. Commun.* 8 (2006) 821–826.
- [162] G.T.-K. Fey, C.-F. Huang, P. Muralidharan, E.S.-S. Chang, *J. Power Sources* 174 (2007) 1147–1151.
- [163] S. Hu, C. Wang, L. Zhou, X. Zeng, L. Shao, J. Zhou, C. Zhou, C. Huang, X. Xi, L. Yang, *Ceram. Int.* 44 (2018) 14995–15000.
- [164] J.-H. Park, J.-M. Kim, J.-S. Kim, E.-G. Shim, S.-Y. Lee, *J. Mater. Chem.* 1 (2013).
- [165] G. Ceder, Y.-M. Chiang, D. Sadoway, M. Aydinol, Y.-I. Jang, B. Huang, *Nature* 392 (1998) 694.
- [166] H. Huang, G.S. Rao, B. Chowdari, *J. Power Sources* 81 (1999) 690–695.
- [167] S. Shi, C. Ouyang, M. Lei, W. Tang, *J. Power Sources* 171 (2007) 908–912.
- [168] D.-G. Tong, Y.-Y. Luo, Y. He, X.-Y. Ji, J.-L. Cao, L.-X. Tang, A.-D. Tang, K.-L. Huang, Q.-Y. Lai, *Mater. Sci. Eng., B* 128 (2006) 220–228.
- [169] S. Xu, R. Jacobs, C. Wolverton, T. Kuech, D. Morgan, *Chem. Mater.* 29 (2017) 1218–1229.
- [170] S.M. Lala, L.A. Montoro, V. Lemos, M. Abbate, J.M. Rosolen, *Electrochim. Acta* 51 (2005) 7–13.
- [171] D. Luo, G. Li, C. Yu, L. Yang, J. Zheng, X. Guan, L. Li, *J. Mater. Chem.* 22 (2012) 22233–22241.
- [172] M. Yoon, Y. Dong, Y. Yoo, S. Myeong, J. Hwang, J. Kim, S.H. Choi, J. Sung, S. J. Kang, J. Li, *Adv. Funct. Mater.* (2019) 1907903.
- [173] R.-Z. Yin, Y.-S. Kim, S.-J. Shin, I. Jung, J.-S. Kim, S.-K. Jeong, *J. Electrochem. Soc.* 159 (2012) A253–A258.
- [174] C. Nithya, R. Thirunakaran, A. Sivashanmugam, S. Gopukumar, *ACS Appl. Mater. Interfaces* 4 (2012) 4040–4046.
- [175] L. Wang, J. Ma, C. Wang, X. Yu, R. Liu, F. Jiang, X. Sun, A. Du, X. Zhou, G. Cui, *Adv. Sci.* (2019) 1900355, 0.
- [176] A. Zhou, J. Xu, X. Dai, B. Yang, Y. Lu, L. Wang, C. Fan, J. Li, *J. Power Sources* 322 (2016) 10–16.
- [177] B. Shen, Q. Liu, L. Wang, G. Yin, P. Zuo, Y. Ma, X. Cheng, C. Du, Y. Gao, *Electrochem. Commun.* 83 (2017) 106–109.
- [178] J. Liu, N. Liu, D. Liu, Y. Bai, L. Shi, Z. Wang, L. Chen, V. Hennige, A. Schuch, *J. Electrochem. Soc.* 154 (2007) A55–A63.
- [179] Y. Ji, P. Zhang, M. Lin, W. Zhao, Z. Zhang, Y. Zhao, Y. Yang, *J. Power Sources* 359 (2017) 391–399.
- [180] J.-N. Zhang, Q. Li, C. Ouyang, X. Yu, M. Ge, X. Huang, E. Hu, C. Ma, S. Li, R. Xiao, W. Yang, Y. Chu, Y. Liu, H. Yu, X.-Q. Yang, X. Huang, L. Chen, H. Li, *Nat. Energy* 4 (2019) 594–603.
- [181] F. Geng, M. Shen, B. Hu, Y. Liu, L. Zeng, B. Hu, *Chem. Commun.* 55 (2019) 7550–7553.
- [182] T. Dong, J. Zhang, G. Xu, J. Chai, H. Du, L. Wang, H. Wen, X. Zang, A. Du, Q. Jia, *Energy Environ. Sci.* 11 (2018) 1197–1203.
- [183] B. Li, Y. Wang, H. Lin, J. Liu, L. Xing, M. Xu, W. Li, *Electrochim. Acta* 141 (2014) 263–270.
- [184] S.S. Zhang, *J. Power Sources* 164 (2007) 351–364.
- [185] E. Quartarone, P. Mustarelli, *Chem. Soc. Rev.* 40 (2011) 2525–2540.